

# Dating and geochemistry of zircon and apatite from rhyolite at the UNESCO geosite Rupnica (Mt. Papuk, northern Croatia) and the relationship to the Sava Zone

Petra Schneider<sup>1,\*</sup>, Dražen Balen<sup>1</sup>, Joachim Opitz<sup>2</sup> and Hans-Joachim Massonne<sup>2</sup>

<sup>1</sup> University of Zagreb, Faculty of Science, Department of Geology, Horvatovac 95, 10000 Zagreb, Croatia; (\*corresponding author: pschneider@geol.pmf.unizg.hr), (drbalen@geol.pmf.unizg.hr)

<sup>2</sup> Universität Stuttgart, Institut für Mineralogie und Kristallchemie (closed), Azenbergstraße 18, 70174 Stuttgart, Germany; (opitz.joachim@web.de, h-j.massonne@imi.uni-stuttgart.de)

doi: 10.4154/gc.2022.19



## Abstract

### Article history:

Manuscript received September 15, 2021  
Revised manuscript accepted April 19, 2022  
Available online June 23, 2022

The Rupnica geosite, a key locality of the UNESCO-protected Papuk Geopark in northern Croatia, is well-known for an excellent exposure of columnar jointing in volcanic rock. This rock is defined as an albite rhyolite that comprises almost pure albite phenocrysts within a fine-grained matrix composed of microphenocrysts of albite, quartz and devitrified volcanic glass. Primary accessory minerals are clinopyroxene, apatite, zircon and magnetite. Haematite, apatite and anatase were found as inclusions in zircon. The albite rhyolite is characterized by a highly siliceous, peraluminous, oxidized (ferroan), dry, alkali-calcic to alkalic composition, with low CaO, MgO, and MnO contents and high  $\text{FeO}_7/(\text{FeO}_7+\text{MgO})$  ratios. Normalized trace element contents display positive anomalies of K, Pb, and Zr as well as negative anomalies of Nb, P, Ti, Ba and Eu, together with an enrichment of light rare-earth elements (REE) relative to heavy REE. Zircon from the rhyolite of Rupnica is characterized by ratios of  $\text{Th}/\text{U}=1.13$  and  $\text{Zr}/\text{Hf}=55$  and contents of  $\text{HfO}_2=1.04$  wt. % typical for an early-stage igneous zircon crystallized from a dry high-temperature magma in a deep magma chamber. Apatite REE patterns show enrichment of light REE over heavy REE and a pronounced Eu anomaly, typical for apatite from granitoids formed in an oxidizing environment. The magma is of A-type and was generated at high temperatures at 800–900 °C by partial melting of lower- to mid-crustal rocks. The age of the albite rhyolite of Rupnica is Late Cretaceous at  $80.8\pm 1.8$  (2 $\sigma$ ) Ma, according to U-Pb dating of zircon, coeval with geochemically similar igneous rocks of Mt. Požeška Gora and Mt. Kozara within the Sava Zone.

**Keywords:** zircon, apatite, rhyolite, Cretaceous, Papuk Geopark, Sava Zone

## 1. INTRODUCTION

Mt. Papuk, situated at the southern edge of the Pannonian basin in northern Croatia (Fig. 1a), is characterized by a complex geological evolution that comprises several orogenic events (JAMIČIĆ, 1983; BALEN et al., 2006, 2013; HORVÁTH et al., 2010). These events led to a variety of rocks and complexes such as granitoids and metamorphic complexes of pre-Variscan, Variscan and Alpine ages. Together with Late Permian–Jurassic sedimentary rocks, these complexes are part of the Tisia Mega-Unit and are surrounded by Neogene and Quaternary sedimentary rocks and sediments of the Pannonian basin (JAMIČIĆ, 1983, 1988; PAMIĆ et al., 1988; PAMIĆ & LANPHERE, 1991a). In addition to the rocks of the Tisia Mega-Unit and those of the Pannonian basin, there are relatively small occurrences of volcanic rocks in the vicinity of the town of Voćin (JAMIČIĆ & BRKIĆ, 1986; JAMIČIĆ et al., 1987, 1989; JAMIČIĆ, 1989; PAMIĆ, 1991). Among them are rocks of the Senonian basalt-rhyolite formation (PAMIĆ, 1997), outcropping at Mt. Papuk near Voćin known as the *Voćin volcanic mass* (PAMIĆ, 1991). These rocks are difficult to distinguish from similar-looking Miocene volcanic rocks in northern Croatia. Based on micropalaeontological records and geological relationships (JAMIČIĆ & BRKIĆ, 1986; JAMIČIĆ et al., 1987, 1989; JAMIČIĆ, 1989; BELAK et al., 2000), it is concluded that the Miocene rocks are related to the evolution of the Pannonian basin. The age of the Voćin volcanic rocks is questionable, because only K-Ar dating on associated basalts (72.8–51.7 Ma, PAMIĆ, 1991) and basalt cores from

drillholes across the Sava depression (83.4–32 Ma, PAMIĆ, 1997) are available. The similar petrography and appearance of the Voćin and Miocene volcanic rocks, as well as the lack of reliable dating led to the above-mentioned age controversies, which also led to different views on the petrogenesis and geodynamic setting of the Voćin rocks.

The Rupnica locality is a key outcrop of the Voćin volcanic rocks with an excellent exposure of columnar jointing (BALEN & PETRINEC, 2014), and is the first protected geosite, i.e. “Geological Monument of Nature”, in Croatia. The exposed rocks are albite and aegirine-albite rhyolites (TAJDER, 1956, 1960). Although these rocks are exposed in a part of the Tisia Mega-Unit, they do not belong to it because volcanic rocks cross-cut through the rocks of the Tisia Mega-Unit (JAMIČIĆ & BRKIĆ, 1986). Intense magmatic activity also took place in the Late Cretaceous within the adjacent geotectonic unit called the Sava (-Vardar) Zone (PAMIĆ, 1993) or Sava suture zone (SCHMID et al., 2008, 2020). The timing of geological processes in this zone and the geochemical features of volcanic rocks also show similarities to the characteristics of the Voćin volcanic rocks at the Rupnica locality. For this reason, we re-evaluated the petrographic and geochemical signatures of the albite rhyolite of Rupnica and determined the trace and isotopic geochemistry of zircon and apatite to unravel and reconstruct the origin, evolution and especially the age of this rock.

Albite rhyolite is a type of acidic high-temperature volcanic rock, which compared to ordinary rhyolite, has high alkali con-

tents (with Na predominating over K) and shows low concentrations of Ca and Mg (TAJDER, 1953, 1960; BALEN & PETRI-NEC, 2014). Moreover, albite rhyolite is often subjected to various alteration processes with zircon being the only remaining primary magmatic and unaltered mineral suitable for dating. In addition, the determination of minor and trace elements in zircon and apatite can provide further geochemical information on magma evolution and petrogenesis. Our U-Th-Pb zircon dating,

which is an improvement of previous age estimates, opens the link to the occurrence of igneous rocks with similar geochemistry and age in the vicinity of the Rupnica site.

## 2. GEOLOGICAL SETTING

### 2.1. Tisia Mega-Unit

The geology of Mt. Papuk is dominated by the Tisia (also Tisza, Tisa) Mega-Unit. This complex and composite unit is regarded

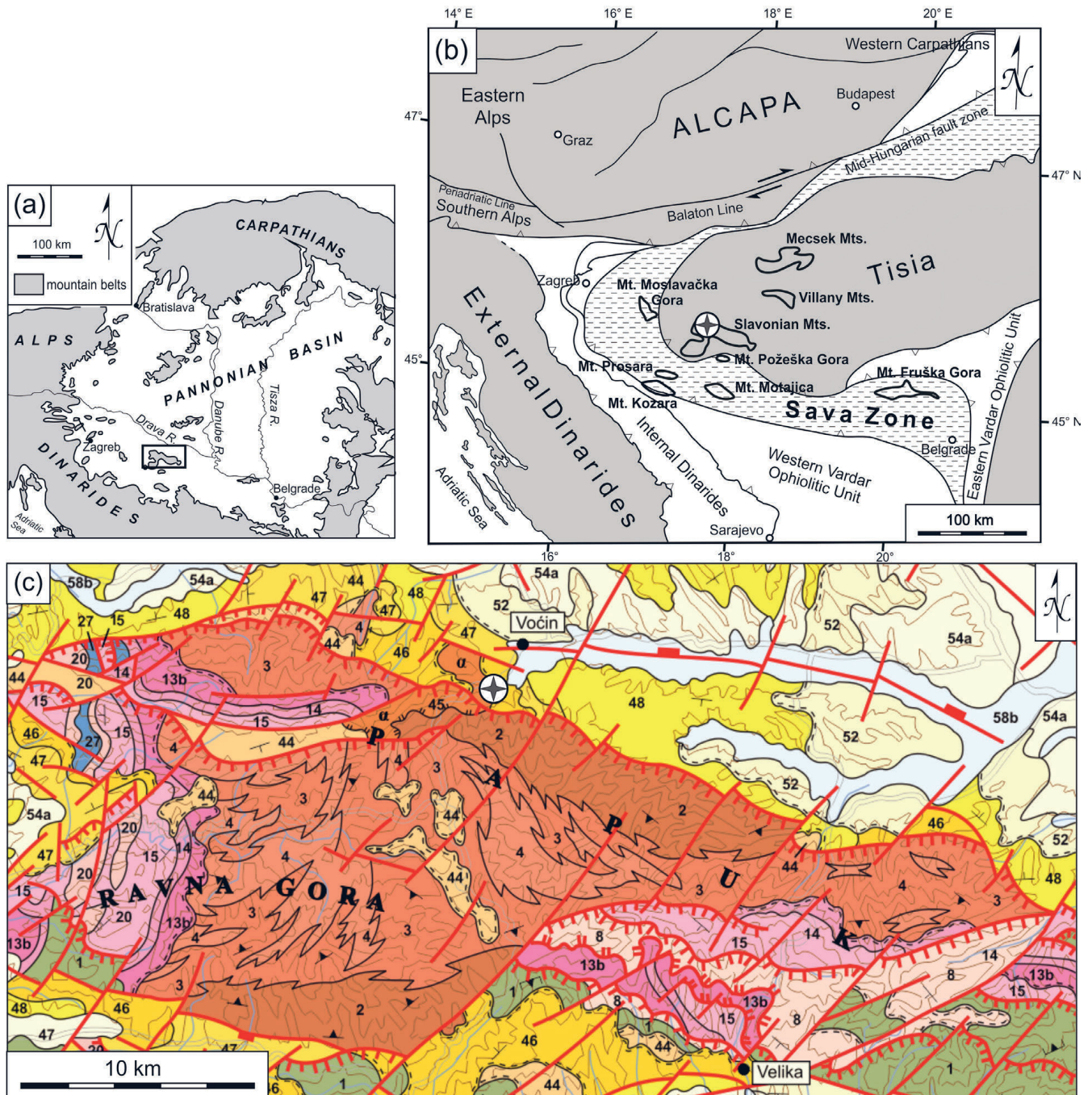


**Figure 1.** Simplified maps of the Dinaride-Alpine-Pannonian region showing: (a) the mountain belts and Pannonian basin and (b) major structural units after SCHMID et al. (2008, 2020). Map modified after LUŽAR-OBERITER et al. (2012). (c) Mt. Papuk geological map (after JAMIČIĆ & BRKIĆ 1986; JAMIČIĆ et al. 1987, 1989; JAMIČIĆ 1989; CROATIAN GEOLOGICAL SURVEY 2009). The position of the study area is marked by the rectangle and circled stars. Legend: 1 – metamorphic rock complex (Precambrian); 2 – progressive metamorphic series (Ordovician-Devonian); 3 – metamorphic rock complex (Ordovician-Devonian); 4 – granitic rocks (Ordovician-Devonian); 8 – Variscan/Hercynian semi-metamorphic complex (Devonian-Permian); 13b – clastic sedimentary deposits (Late Permian); 14 – clastic sedimentary deposits and carbonates (Early Triassic); 15 – carbonate deposits (Middle Triassic); 27 – limestones (Jurassic); 44 – clastic sedimentary deposits and carbonates (Miocene,  $M_{2,3}$ ); 46 – “litavac” (bioclastic beech carbonate) and clastic sedimentary deposits with volcanic rocks (Miocene,  $M_4$ ); 47 – carbonate clastic deposits (Miocene,  $M_{5,6}$ ); 48 – clastic sedimentary rocks and coal (Miocene,  $M_7$ ); 52 – clastic deposits (Plio-Quaternary); 54a – loess (Pleistocene); 58b – alluvial deposits (Holocene);  $\alpha$  – andesites and rhyolites (Miocene,  $M_{3,4}$ ).

as a continental fragment which rifted and drifted away from Europe in the Middle Jurassic as a consequence of kinematically linked opening of the easternmost branch of the Alpine Tethys Ocean (Ceahlau-Severin Ocean) (SCHMID et al., 2020). The final emplacement of the Tisia Mega-Unit into the present-day configuration took place during the Palaeogene and Miocene, i.e. after its internal structuring, which mainly occurred during a Cretaceous orogeny (SCHMID et al., 2020). Only small parts of this unit are exposed in rare isolated and rather small so-called *inselbergs* within the Pannonian basin, such as the Mecsek and Villany Mts. of Hungary, the northern Apuseni Mts. in Romania and the Slavonian Mts. in Croatia (Fig. 1b). The Slavonian Mts. include the Mt. Papuk area where pre-Variscan, Variscan and Alpine igneous and metamorphic rocks crop out (Fig. 1c; BALEN et al., 2015, 2018; BIŠEVAC et al., 2010; HORVAT et al., 2018; SLOVENEK et al., 2020).

## 2.2. Sava Zone

The western branch of the Neotethys Ocean was closed through convergence of the Adria microplate (Dinarides) and Europe (Tisia). This convergence caused the formation of a suture zone named the Sava-Vardar Zone (PAMIĆ, 2002), Sava Zone or Sava suture zone (SCHMID et al., 2008, 2020). The Sava Zone is a complex belt comprising ophiolites and related igneous, metamorphic and sedimentary rocks, including Cretaceous to Eocene deep water sediments and flysch. Late Cretaceous ophiolites represent the structurally lowermost unit of the Sava Zone. This zone runs from Zagreb towards Belgrade, and then further to the south through the Vardar Zone into Greece (Fig. 1b; SCHMID et al., 2008; USTASZEWSKI et al., 2010). The northwestern end of the Sava Zone close to Zagreb sharply turns into the SW-NE strike of the Mid-Hungarian fault zone and is further buried below the Cenozoic cover of the Pannonian basin (SCHMID et al., 2020). The formation age of the Sava Zone ranges from the Cretaceous to the Early Palaeogene until the final collision of the Dinarides with the Tisia Mega-Unit (PAMIĆ, 2002). The relatively rare late Mesozoic and Cenozoic igneous rocks within the Sava Zone are related to magmatism along the Europe-Adria suture zone. Known occurrences of these rocks (Fig. 1b) are in northern Bosnia (Mts. Kozara, Prosara and Motajica), northern Serbia (Mt. Fruška Gora) and eastern Croatia (Mts. Požeška Gora and Moslavačka Gora) (e.g. SCHMID et al., 2008).

## 2.3. Senonian basalt-rhyolite formation

In part of the Slavonian Mts. PAMIĆ (1997) described a Senonian basalt-rhyolite formation including A-type granites. Rocks of this formation crop out in the areas of Mt. Požeška Gora (with the only known surface occurrence of A-type granite at the Gradski Vrhovci locality; PAMIĆ, 1987; PAMIĆ & LANPHERE, 1991a) and Mt. Papuk. The volcanic rocks at the latter locality, the so-called *Voćin volcanic mass* (PAMIĆ, 1997), are situated at the northern slopes of Mt. Papuk, near the town of Voćin, and include the rocks from the Rupnica locality. The *Voćin volcanic mass* consists of basalts, rhyolites and pyroclastic rocks, covers an area of ~10 km<sup>2</sup> (PAMIĆ, 1991), and penetrates the igneous, metamorphic and sedimentary rocks of surrounding complexes (Fig. 1c). PAMIĆ (1991) proposed a Late Cretaceous age for the volcanic rocks in the immediate area of Voćin, while the volcanic and pyroclastic rocks in the wider area were considered to be Miocene in age (JAMIČIĆ et al., 1987, 1989; BELAK et al., 2000). The whole-rock K-Ar dating at 72.8–51.7 Ma presented in PAMIĆ (1991) was conducted on basalts. The older ages were obtained

on relatively fresh basalts, whereas the younger ones resulted from the study of altered basalts (spilites). Younger ages were interpreted as a consequence of a loss of radiogenic Ar, possibly during the younger volcanic activity in the area, which also produced spatially associated basalts. Furthermore, K-Ar dating was performed on basalt cores from drillholes across the Sava depression (PAMIĆ, 1997) with ages between 83.4 and 32 Ma.

## 2.4. A-type granite of Mt. Požeška Gora

The A-type granite of Mt. Požeška Gora (PAMIĆ, 1987; PAMIĆ et al., 1988/89; PAMIĆ & LANPHERE, 1991b) has been reinvestigated in detail by BALEN et al. (2020), who confirmed a Late Cretaceous age (83.6±1.5 Ma) by U-Th-Pb dating on zircon. This recent study revealed the significance of this rather small granite body because it marks the activation of deep faults in an extensional tectonic environment at the suture zone, where the subduction of the Adria plate under the European plate took place. Therefore, this A-type granite indicates the local tectonic transition from compression to extension. The idea of a connection between the Late Cretaceous (Senonian) volcanic masses at Mt. Požeška Gora and Mt. Papuk was already postulated by PAMIĆ (1997). Therefore, it is of interest to compare the geochemical features of rhyolite at the Rupnica site, its accessory minerals and the crystallization age of zircon, with the same features of the A-type granite from Mt. Požeška Gora.

## 2.5. Miocene volcanic rocks

A detailed description of volcanic rocks from the northwestern part of Mt. Papuk (including Voćin and its surroundings) can be found in LUGOVIĆ (1983), where an overview of the age constraints based on earlier reports is given. In these historical papers (STUR, 1861/62; KOCH, 1919; POLJAK, 1939), besides details on field relationships, the prevailing opinion is that these rocks are of Miocene age.

In the Basic Geological Map of Croatia M 1:300,000 (CROATIAN GEOLOGICAL SURVEY, 2009) volcanic rocks at Voćin and its surroundings are described as andesites and rhyolites of Miocene age (Fig. 1c), as it was postulated in the Basic Geological Map of SFRY 1:100,000, sheets Orahovica and Daruvar (JAMIČIĆ & BRKIĆ, 1986; JAMIČIĆ et al., 1987, 1989; JAMIČIĆ, 1989). The contact of the Voćin volcanic rocks with the Triassic and Late Cretaceous deposits is described as tectonic. According to the interpretation in the above mentioned explanatory notes, the volcanic activity was accompanied by sedimentary processes related to the evolution of the Pannonian basin.

## 3. ANALYTICAL METHODS

### 3.1. Whole-rock chemistry

From 20 collected homogeneous samples at the Rupnica geosite, 3 samples plus 1 used in BALEN & PETRINEK (2014) were selected for whole-rock geochemistry. These samples were crushed in a jaw crusher, powdered in an agate mill, and analysed at the Bureau Veritas Commodities Canada Ltd. (Vancouver) by inductively coupled plasma mass spectrometry (ICP-MS; trace elements including rare-earth elements (REE)) and inductively coupled plasma emission spectrometry (ICP-ES; major elements). Powders were air-dried and sieved through a 0.125 mm stainless-steel screen. The sample preparation included the splitting of 0.2 g rock powder each for LiBO<sub>2</sub>/Li<sub>2</sub>B<sub>4</sub>O<sub>7</sub> fusion for ICP-ES and ICP-MS. Natural rocks of known composition and pure quartz were used as reference materials. The analytical accuracy was

**Table 1.** Results of the whole-rock analyses of major (wt. %) and trace (ppm) elements with characteristic element ratios and zircon saturation temperatures (ZST) after WATSON & HARRISON (1983) and GERVASONI et al. (2016) for selected samples of rhyolite of Rupnica. The compositions were determined with ICP-MS and ICP-ES. Sample 1 is from BALEN & PETRINEC (2014).

Major elements (wt. %)	Sample 1 RUP	Sample 2 Rupnica 3	Sample 3 Rup4	Sample 4 Rup7	d.l. (wt. %)	MIN	MAX	Mean
SiO <sub>2</sub>	66.41	66.83	69.5	68.27	0.01	66.41	69.50	67.75
TiO <sub>2</sub>	0.45	0.42	0.41	0.41	0.01	0.41	0.45	0.42
Al <sub>2</sub> O <sub>3</sub>	16.7	15.61	15.35	15.53	0.01	15.35	16.70	15.80
Fe <sub>2</sub> O <sub>3</sub>	3.87	3.72	3.53	4.22	0.04	3.53	4.22	3.84
MnO	0.03	0.07	0.05	0.04	0.01	0.03	0.07	0.05
MgO	0.53	0.48	0.27	0.38	0.01	0.27	0.53	0.42
CaO	0.36	1.48	0.35	0.36	0.01	0.35	1.48	0.64
Na <sub>2</sub> O	5.6	5.29	5.27	5.22	0.01	5.22	5.60	5.35
K <sub>2</sub> O	3.41	2.91	3.47	3.23	0.01	2.91	3.47	3.26
P <sub>2</sub> O <sub>5</sub>	0.12	0.11	0.1	0.11	0.01	0.10	0.12	0.11
LOI	2.40	2.90	1.60	2.10	0.01	1.60	2.90	2.25
Total	99.88	99.82	99.9	99.87		99.82	99.90	99.87
Trace elements (ppm)	(ppm)							
As	3.2	1.2	1.4	8.5	0.5	1.2	8.5	3.575
Au (ppb)	0.3	1.9	32.4	28.1	0.5 (ppb)	0.3	32.4	15.7
Ba	548	459	492	512	1	459	548	503
Be	4	2	2	3	1	2	4	2.75
Co	1.3	2.7	0.8	2.8	0.2	0.8	2.8	1.9
Cs	0.4	<0.1	0.5	0.7	0.1	0.4	0.7	0.5
Cu	1.3	16.2	7.3	14.7	0.1	1.3	16.2	9.9
Ga	20	21	18	16	0.5	16.4	20.8	18.6
Hf	9.0	9.5	7.6	7.9	0.1	7.6	9.5	8.5
Mo	0.6	0.6	0.5	0.5	0.1	0.5	0.6	0.6
Nb	26	27	22	25	0.1	22	27	25
Ni	1.5	2.9	0.9	2.3	0.1	0.9	2.9	1.9
Pb	3.7	8.4	11.0	14.6	0.1	3.7	14.6	9.4
Rb	45	44	55	52	0.1	44	55	49
Sb	<0.1	0.2	0.5	0.4	0.1	0.2	0.5	0.4
Sc	7	7	6	7	1	6	7	7
Sn	4	4	4	4	1	4	4	4
Sr	134	175	129	117	0.5	117	175	139
Ta	1.7	1.7	1.6	1.4	0.1	1.4	1.7	1.6
Th	9.4	9.8	8.8	7.7	0.2	7.7	9.8	8.9
U	2.0	2.1	2.0	2.1	0.1	2.0	2.1	2.1
V	11	17	12	14	8	11	17	13.5
W	1.5	2.0	1.3	1.5	0.5	1.3	2.0	1.6
Y	32	37	29	32	0.1	29	37	32
Zn	59	70	48	66	1	48	70	61
Zr	354	386	329	339	0.1	329	386	352
La	29	33	29	18	0.1	18	33	27
Ce	63	60	55	49	0.1	49	63	57
Pr	6.6	6.9	6.6	4.4	0.02	4.4	6.9	6.1
Nd	25	27	26	17	0.3	17	27	24
Sm	5.6	5.7	5.6	4.1	0.05	4.1	5.7	5.3
Eu	1.4	1.4	1.3	1.0	0.02	1.0	1.4	1.3
Gd	5.9	6.4	5.1	5.2	0.05	5.1	6.4	5.6
Tb	1.1	1.1	0.9	0.9	0.01	0.9	1.1	1.0
Dy	6.0	6.4	5.8	5.6	0.05	5.6	6.4	5.9
Ho	1.2	1.4	1.2	1.1	0.02	1.1	1.4	1.2
Er	3.6	4.2	3.2	3.4	0.03	3.2	4.2	3.6
Tm	0.6	0.6	0.5	0.5	0.01	0.5	0.6	0.5
Yb	3.4	3.9	3.3	3.5	0.05	3.3	3.9	3.5
Lu	0.5	0.6	0.5	0.6	0.01	0.5	0.6	0.5

Table 1. continued.

	Sample 1 RUP	Sample 2 Rupnica 3	Sample 3 Rup4	Sample 4 Rup7	MIN	MAX	Mean
MI	0.87	0.87	0.92	0.91	0.87	0.92	0.89
A/CNK	1.24	1.08	1.19	1.23	1.08	1.24	1.19
A/NK	1.29	1.32	1.24	1.29	1.24	1.32	1.28
K <sub>2</sub> O/Na <sub>2</sub> O mol	0.40	0.36	0.43	0.41	0.36	0.43	0.40
Ba/Rb	12.1	10.6	9.0	9.8	9.0	12.1	10.4
10000-Ga/Al	2.2	2.5	2.2	2.0	2.0	2.5	2.2
Zr/Hf	39	41	43	43	39	43	42
Y/Ho	26	27	25	28	25	28	26
(La/Yb) <sub>N</sub>	5.75	5.70	5.92	3.47	3.47	5.92	5.21
(La/Sm) <sub>N</sub>	3.26	3.64	3.26	2.76	2.76	3.64	3.23
(Gd/Yb) <sub>N</sub>	1.40	1.32	1.25	1.20	1.20	1.40	1.29
Ce/Ce*	1.10	0.96	0.96	1.33	0.96	1.33	1.08
Eu/Eu*	0.74	0.71	0.74	0.66	0.66	0.74	0.71
Σ REE	152	159	142	115	115	159	142
M	1.33	1.50	1.33	1.27	1.27	1.50	1.36
T <sub>WH</sub> (°C)	866	860	858	867	858	867	863
G	8.20	7.81	8.98	8.51	7.81	8.98	8.38
T <sub>G</sub> (°C)	789	778	798	790	778	798	789

d.l. = detection limit; LOI = loss on ignition; MI (mafic index) =  $\text{FeO}_{7}/(\text{FeO}_{7}+\text{MgO})$ ; A/CNK =  $\text{Al}_2\text{O}_3/(\text{CaO}+\text{Na}_2\text{O}+\text{K}_2\text{O})$  in mol%; A/NK =  $\text{Al}_2\text{O}_3/(\text{Na}_2\text{O}+\text{K}_2\text{O})$ ; M (cation ratio) =  $(\text{Na}+\text{K}+2\text{Ca})/\text{Al-Si}$ ; G =  $(3\text{-Al}_2\text{O}_3+\text{SiO}_2)/(\text{Na}_2\text{O}+\text{K}_2\text{O}+\text{CaO}+\text{MgO}+\text{FeO})$  in molar proportions; T<sub>WH</sub> and T<sub>G</sub> – Zircon saturation temperatures after WATSON & HARRISSON (1983) and GERVASONI et al. (2016), respectively.

controlled using internal geological reference materials, the compositions of which are comparable to the rocks in this study (STDGS311-1, STD GS910-4, STD DS10, STD OREAS45EA, STD SO-19). Detection limits are shown in Table 1. Reference materials were certified in-house by analysis with CANMET Certified Reference Materials. Loss on ignition (LOI) was determined by weight difference before and after 4 hours ignition at 1000 °C. Geochemical data and diagrams are recalculated and handled with the GCDkit software (JANOŠEK et al., 2006).

### 3.2. Scanning electron microscopy

Zircon was separated from the rhyolite (sample Rupnica 3) by a standard procedure of extraction from the host rock (crushing of the rock, sieving, heavy-liquid separation with sodium polytungstate and magnetic separation) and analysed using scanning electron microscopy at the Slovak Academy of Sciences, Earth Science Institute, Laboratory of electron microscopy in Banská Bystrica, in order to detect the external morphology of individual zircon grains. The analyses were performed with a JEOL JSM-6390LV equipped with a secondary electron detector for imaging and an acceleration voltage of 20 kV. The specimens were coated with gold.

### 3.3. Raman spectroscopy

Separated zircon grains were also analysed with the aid of micro-Raman spectroscopy in order to characterize the inclusions in zircon. This spectroscopy was performed at the Slovak Academy of Sciences, Earth Science Institute, Laboratory of vibration spectroscopy in Banská Bystrica with a Horiba Jobin-Yvon LabRam HR 800 spectrometer equipped with a Czerny-Turner monochromator, 600 grooves per mm grating, and a Peltier-cooled charge-coupled device detector coupled to an Olympus BX41 microscope with a long working distance 100×/0.8 objective. Zircon crystals were irradiated by a He–Ne (633 nm) laser

with a power of ~3 mW. A frequency-doubled Nd:YAG (532 nm) laser was only used for verifying possible luminescence effects. The Rayleigh line (0 cm<sup>-1</sup>) and emission bands of Ne glow lamps were used for calibration. Wave-number accuracy and lateral resolution were better than 0.8 cm<sup>-1</sup> and 1 μm, respectively. The spectral resolution was ~3.6 cm<sup>-1</sup> (red spectral range). The spectra of the unknown phases were collected in the range of 60–4000 cm<sup>-1</sup> to additionally cover the region of OH-stretching bands.

### 3.4. Laser ablation – inductively coupled plasma – mass spectrometry (LA-ICP-MS)

Isotopic concentrations of selected elements in zircon were determined by LA-ICP-MS. Analyses were performed at the Institut für Mineralogie und Kristallchemie, Universität Stuttgart (Germany), using an AGILENT 7700 mass spectrometer after laser ablation with a CETAC LSX-213 laser system. The diameter of the ablated spots was 25 μm. The laser energy was set to 100 % of the maximum (100 % = 4 mJ at a spot diameter of 150 μm) at a laser pulse frequency of 10 Hz and 330 (for elemental concentrations) or 375 (for dating) laser pulses per analysis. A mixed He and Ar gas flow with 500 ml/min and 800 ml/min, respectively, served as carrier of the ablated material into the ICP-MS system. Zircon grains separated from the rhyolite were mounted in an epoxy resin and polished approximately to their centres. The details of the data evaluation methods and corrections are given in BALEN et al. (2020).

#### 3.4.1. Zircon chemical analysis

Glass standards for the determination of elemental concentrations in zircon were the following: DLH7 and DLH8 from P&H Developments Ltd. and NIST612 and NIST610 from National Institute of Standards and Technology, USA. The validity of the calibration, data evaluation, and reproducibility were checked with the

**Table 2.** Chemistry of zircon from the rhyolite of Rupnica determined by LA-ICP-MS with characteristic element ratios and detection limits (d.l.). Elemental mass concentrations and detection limits are given in ppm. Ti-in-zircon temperature was calculated for selected grains after WATSON et al. (2006). b.d.l. – below detection limit.

Element	Grain 1a	Grain 2a	Grain 3a	Grain 4a	Grain 5a	Grain 6a	Grain 7a	Grain 8a	Grain 9a	Grain 10a	Grain 11a	Grain 12a	Grain 13a	Grain 14a	d.l.	MIN	MAX	Mean	Median
Ba	0.7	1.0	0.9	0.8	1.3	5.0	0.9	1.5	1.0	1.6	1.7	4.2	13.1	3.9	0.4	0.7	13	2.7	1.4
Ca	20140	12592	8871	b.d.l.	14409	34730	27978	15079	15174	32291	6227	3744	4119	25624	770	3744	34730	16998	15079
Cr	3.5	3.8	2.1	2.7	3.2	3.6	2.0	3.5	3.9	3.6	3.0	2.9	3.9	2.1	2	2.0	3.9	3.1	3.3
Fe	652	426	751	323	356	4518	2119	683	270	954	389	347	2006	763	33	270	4518	1040	667
Ga	1.1	b.d.l.	b.d.l.	b.d.l.	1.1	2.6	1.3	3.1	0.6	1.1	1.5	b.d.l.	1.0	1.3	0.4	0.6	3.1	1.5	1.2
Hf	9791	7283	11511	9348	9113	7834	9405	11342	7646	7447	9411	6436	7771	8635	0.3	6436	11511	8784	8874
Mn	52	28	24	5.9	45	103	137	53	67	78	13	9.0	8.0	7.4	2	5.9	137	55	52
Nb	9.0	4.4	7.6	9.9	15	28	8.5	25	13	7.9	13	9.0	8.0	7.4	0.04	4.4	28	12	9.0
P	8280	6539	3402	911	10097	12972	13346	9697	6884	14372	2529	3182	2592	12590	148	911	14372	7671	7582
Pb	4.2	2.3	5.6	10	7.2	8.9	5.0	11	5.1	3.6	6.5	12	117	3.5	0.2	2.3	117	14	6.1
Si	151400	151400	151400	151400	151400	151400	151400	151400	151400	151400	151400	151400	151400	151400	1223	151400	151400	151400	151400
Sn	1.0	b.d.l.	b.d.l.	b.d.l.	2.0	1.3	1.3	b.d.l.	1.0	1.0	1.2	b.d.l.	b.d.l.	b.d.l.	0.8	1.0	2.0	1.2	1.1
Sr	23	14	6.6	1.6	35	18	31	17	12	29	12	4.5	4.4	27	0.1	1.6	35	17	16
Ta	2.8	1.2	2.1	2.4	3.3	2.8	2.6	5.2	2.7	1.3	3.3	1.8	2.0	1.9	0.04	1.2	5.2	2.5	2.5
Th	405	107	302	425	799	871	539	1411	558	272	715	337	350	348	0.1	107	1411	531	415
Ti	78	152	34	19	21	490	41	38	21	605	108	55	26	89	2	19	605	127	48
U	400	137	291	380	667	536	466	958	505	282	588	342	336	320	0.1	137	958	443	390
V	0.6	0.6	0.2	0.3	0.1	1.6	0.9	0.3	0.2	0.7	0.2	0.3	0.6	0.3	0.2	0.1	1.6	0.5	0.3
Y	3625	1178	3656	3710	6154	4465	3570	5997	5223	3127	4920	3577	2315	2975	0.2	1178	6154	3892	3641
Zn	7.9	13	23	262	9.9	29	15	14	7.5	22	13	616	1689	7.3	2	7.3	1689	195	14
Zr	452114	432394	488423	525378	480423	446724	491755	508904	481539	453172	486556	438820	451241	467646	8	432394	525378	471792	474034
La	63	23	17	3.5	75	119	99	63	54	95	89	20	14	73	0.06	3.5	119	58	63.0
Ce	149	72	58	25	207	372	252	236	134	223	248	61	37	177	0.08	25	372	161	163
Pr	20	7.6	5.3	1.5	23	52	40	30	14	29	34	6.3	3.7	25	0.03	1.5	52	21	21
Nd	123	39	32	14	139	257	172	170	76	128	174	29	21	127	0.26	14	257	107	125
Sm	44	13	22	17	80	71	49	77	44	45	68	19	19	40	0.29	13	80	43	44
Eu	5.5	1.7	3.9	2.7	9.9	7.8	6.0	8.3	6.3	5.1	6.8	2.7	3.2	4.4	0.07	1.7	9.9	5.3	5.3
Gd	114	27	94	86	235	156	129	227	157	100	164	80	69	89	0.22	27	235	123	107
Tb	32	9.0	28	28	65	40	36	59	47	28	42	24	22	27	0.03	9.0	65	35	30
Dy	395	110	291	341	693	403	369	558	527	328	534	254	249	339	0.23	110	693	385	355
Ho	143	46	127	127	219	151	129	182	190	117	167	89	86	118	0.04	46	219	135	128
Er	641	229	670	593	869	652	570	884	787	533	741	400	371	495	0.11	229	884	602	617
Tm	126	47	141	114	159	123	121	177	153	103	145	82	71	101	0.05	47	177	119	122
Yb	1120	444	1122	944	1377	983	1071	1517	1239	874	1235	711	585	877	0.29	444	1517	1007	1027
Lu	222	87	226	181	277	170	203	302	214	159	224	136	112	170	0.04	87	302	192	192
Sum REE	3196	1155	2836	2479	4427	3557	3246	4490	3642	2769	3870	1914	1662	2662		1155	4490	2993	3016
Sum oxides (wt %)	100.44	95.38	102.78	105.75	104.28	103.44	108.24	108.54	103.36	103.38	102.04	94.62	96.57	104.01		94.62	108.54	102.35	103.37
HfO <sub>2</sub>	11547	8588	13574	11024	10747	9239	11092	13376	9017	8782	11098	7590	9164	10184		7590	13574	10372	10747
Y <sub>2</sub> O <sub>3</sub>	4603	1495	4643	4711	7815	5670	4534	7616	6633	3972	6248	4543	2940	3778		1495	7815	5033	4643
Th/U	1.01	0.78	1.04	1.12	1.20	1.62	1.16	1.47	1.11	0.97	1.22	0.99	1.04	1.09		0.78	1.62	1.13	1.10
Zr/Hf	46	59	42	56	53	57	52	45	63	61	52	68	58	54		42	68	55	55.2
Nb/Ta	3.2	3.7	3.7	4.0	4.5	10.0	3.3	4.8	4.8	6.3	4.0	5.0	4.0	3.9		3.2	10	4.7	4.0
Ce/Ce*	1.01	1.31	1.47	2.63	1.20	1.14	0.96	1.31	1.17	1.02	1.09	1.31	1.24	1.00		0.96	2.63	1.27	1.19
Eu/Eu*	0.24	0.28	0.26	0.22	0.22	0.23	0.23	0.19	0.23	0.23	0.20	0.21	0.27	0.23		0.19	0.28	0.23	0.23
La <sub>N</sub> /Yb <sub>N</sub>	0.04	0.03	0.01	0.00	0.04	0.08	0.06	0.03	0.03	0.07	0.05	0.02	0.02	0.06		0.00	0.08	0.04	0.04
La <sub>N</sub> /Sm <sub>N</sub>	0.90	1.11	0.49	0.13	0.59	1.05	1.27	0.51	0.77	1.33	0.82	0.66	0.46	1.15		0.13	1.33	0.80	0.80
Gd <sub>N</sub> /Yb <sub>N</sub>	0.08	0.05	0.07	0.07	0.14	0.13	0.10	0.12	0.10	0.09	0.11	0.09	0.10	0.08		0.05	0.14	0.09	0.09
Ti-in-zircon (°C)				801					812				831			801	831	814	812

reference materials Diorite (DRN) and Zinnwaldite (ZW-C) from Service d'Analyses des Roches et des Minéraux du CNRS. Relative elemental concentrations were calculated from the abundance of the corresponding isotopes, assuming natural isotopic distributions and individual calibration factors, which were determined under the same experimental conditions. Absolute elemental concentrations were calculated on the basis of the known absolute elemental concentration of an internal reference element.

For zircon chemical analysis, the following isotopes were monitored:  $^{28,29}\text{Si}$ ,  $^{31}\text{P}$ ,  $^{42,44}\text{Ca}$ ,  $^{45}\text{Sc}$ ,  $^{49}\text{Ti}$ ,  $^{51}\text{V}$ ,  $^{52}\text{Cr}$ ,  $^{55}\text{Mn}$ ,  $^{56,57}\text{Fe}$ ,  $^{59}\text{Co}$ ,  $^{60}\text{Ni}$ ,  $^{66}\text{Zn}$ ,  $^{71}\text{Ga}$ ,  $^{88}\text{Sr}$ ,  $^{89}\text{Y}$ ,  $^{90,91}\text{Zr}$ ,  $^{93}\text{Nb}$ ,  $^{118}\text{Sn}$ ,  $^{137}\text{Ba}$ ,  $^{139}\text{La}$ ,  $^{140}\text{Ce}$ ,  $^{141}\text{Pr}$ ,  $^{146}\text{Nd}$ ,  $^{147,149}\text{Sm}$ ,  $^{151,153}\text{Eu}$ ,  $^{157}\text{Gd}$ ,  $^{159}\text{Tb}$ ,  $^{161,163}\text{Dy}$ ,  $^{165}\text{Ho}$ ,  $^{166}\text{Er}$ ,  $^{169}\text{Tm}$ ,  $^{172}\text{Yb}$ ,  $^{175}\text{Lu}$ ,  $^{177,178}\text{Hf}$ ,  $^{181}\text{Ta}$ ,  $^{208}\text{Pb}$ ,  $^{232}\text{Th}$  and  $^{238}\text{U}$ . All elemental concentrations were calculated relative to  $\text{Si}=15.14$  wt. %, a value which is taken as an internal reference value in zircon, because Si is least likely to be replaced by other elements in the zircon structure. Therefore, the mean value of Si, as derived from the isotopes  $^{28,29}\text{Si}$ , was set to 151,400 ppm. The

calculated elemental concentrations are presented in Table 2. The concentrations of elements, which are usually not incorporated in zircon, were either very near to the detection limit or clearly elevated and therefore ascribed to inclusions in zircon.

#### 3.4.2. Apatite chemical analysis

Through the process of zircon separation with sodium polytungstate, grains of apatite were also successfully separated due to their relatively high specific gravity. Separated grains were used for chemical analysis of apatite, for which the same set of isotopes were monitored as for the chemical analyses of zircon.

All elemental concentrations were calculated relative to  $\text{P}=18.25$  wt. %, a value which is taken as a reference value in apatite, with the assumption that P is hardly replaced by some other elements in the apatite structure. Therefore, the P concentration, derived from the isotope  $^{31}\text{P}$ , was set to 182,500 ppm. The calculated elemental concentrations are summarized in Table 3. The

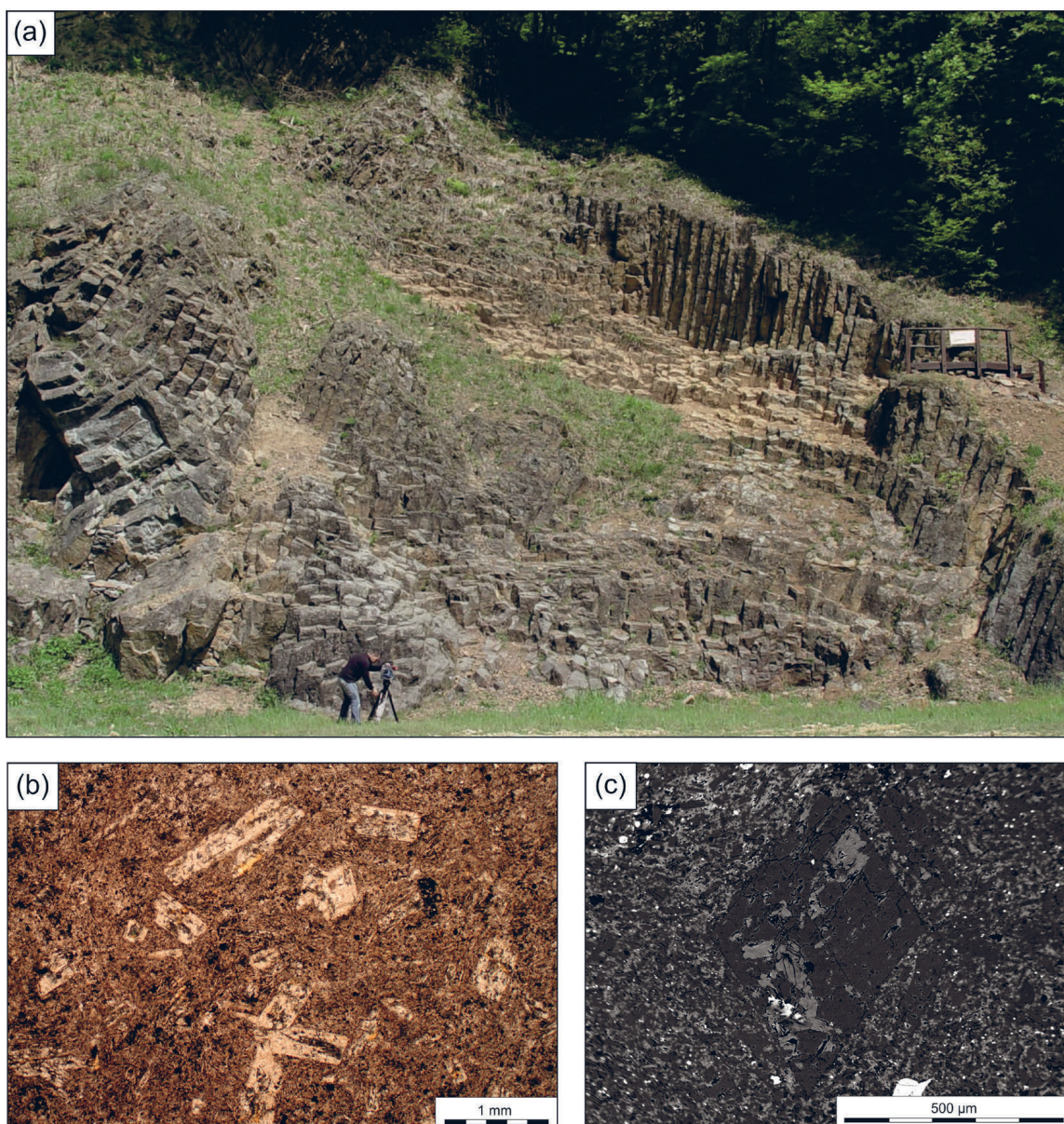


**Figure 2.** (a) Columnar jointing of albite rhyolite at the Rupnica geosite; person as scale; (b) plain-polarized transmitted-light photomicrograph of a typical microfabric of the rhyolite of Rupnica taken from a thin section of the Rupnica 3 sample; (c) backscattered electron image displaying the texture of the rhyolite of Rupnica. The centre of the image shows an albite phenocryst.

**Table 3.** Chemistry of apatite from the rhyolite of Rupnica determined by LA-ICP-MS with characteristic element ratios and detection limits (d.l.). Elemental mass concentrations and detection limits are given in ppm. b.d.l. – below detection limit.

Element	Grain 1	Grain 2	Grain 3	Grain 4	Grain 5	Grain 6	Grain 7	Grain 8	Grain 9	Grain 10	Grain 11	d.l.	MIN	MAX	Mean	Median
Ba	4.9	7.0	5.2	6.8	5.1	4.0	4.8	5.8	6.1	5.9	7.5	0.49	4.0	7.5	5.7	5.8
Ca	449619	446272	379487	431069	403360	374870	347709	417405	407031	421231	440466	936	347709	449619	410774	417405
Co	b.d.l.	0.31	0.21	0.25	0.35	b.d.l.	b.d.l.	0.36	0.66	0.22	0.20	0.20	0.20	0.66	0.32	0.28
Cr	3.9	3.0	2.2	2.3	2.4	2.4	4.3	3.1	4.3	2.8	3.0	1.9	2.2	4.3	3.1	3.0
Fe	3189	3267	14	23	1459	b.d.l.	b.d.l.	65	2584	427	b.d.l.	11	14	3267	1378	943
Ga	11	17	17	12	6.7	12	11	11	14	17	12	0.35	6.7	17	13	12
Hf	0.41	8.1	0.65	0.24	0.37	1.5	b.d.l.	1.1	2.2	0.83	0.24	0.22	0.24	8	1.6	0.74
Mn	750	844	892	851	793	1022	721	817	1066	1016	801	1.6	721	1066	870	844
Nb	1.2	1.1	0.14	0.09	12	0.06	0.10	0.26	2.0	5.4	b.d.l.	0.06	0.06	12	2.3	0.70
P	182500	182500	182500	182500	182500	182500	182500	182500	182500	182500	182500	125	182500	182500	182500	182500
Pb	2.5	3.6	2.1	2.2	3.6	1.1	1.7	1.9	2.3	3.0	2.0	0.20	1.1	3.6	2.4	2.2
Sc	b.d.l.	2.0	3.5	1.6	2.5	2.4	b.d.l.	b.d.l.	2.0	b.d.l.	b.d.l.	1.6	1.6	3.5	2.3	2.2
Si	4193	4916	4687	4914	4482	3234	3081	3987	7267	5076	4233	1239	3081	7267	4552	4482
Sn	1.1	b.d.l.	b.d.l.	b.d.l.	2.1	b.d.l.	1.8	b.d.l.	b.d.l.	1.1	b.d.l.	0.97	1.1	2.1	1.5	1.4
Sr	386	382	3799	396	526	420	298	458	387	501	430	0.09	298	526	415	396
Ta	0.04	0.04	b.d.l.	b.d.l.	0.36	0.05	b.d.l.	b.d.l.	0.07	0.11	b.d.l.	0.03	0.04	0.36	0.11	0.06
Th	15	24	25	15	12	15	12	12	19	21	11	0.07	11	25	16	15
Ti	146	162	14	23	1459	3.6	b.d.l.	65	2584	427	3.3	3.2	3.3	2584	489	105
U	5.8	8.5	9.5	5.7	4.6	5.9	5.0	4.9	8.6	8.0	3.8	0.09	3.8	9.5	6.4	5.8
V	3.2	3.5	0.9	3.3	5.0	0.3	3.4	7.6	8.2	2.4	7.5	0.21	0.3	8.2	4.1	3.4
Y	1029	1617	1346	1019	693	951	954	980	1172	1530	1052	0.12	693	1617	1122	1029
Zn	5.1	12	8.1	10	9.8	7.1	5.9	11	29	34	8.3	2.9	5.1	34	13	10
Zr	47	478	38	13	18	183	9.1	42	174	57	12	0.47	9.1	478	97	42
La	766	1265	1276	891	539	854	717	767	1194	1231	969	0.07	539	1276	952	891
Ce	1750	3089	2901	2258	1339	2134	1793	1805	2772	2909	2149	0.10	1339	3089	2263	2149
Pr	231	450	379	325	196	282	246	263	356	403	275	0.07	196	450	310	282
Nd	1139	1921	1901	1582	962	1417	1254	1254	1791	2106	1229	0.49	962	2106	1505	1417
Sm	271	495	444	344	251	375	313	311	414	528	298	0.41	251	528	368	344
Eu	34	49	43	45	56	53	32	41	44	54	41	0.10	32	56	45	44
Gd	284	458	413	334	288	325	271	309	403	428	320	0.45	271	458	349	325
Tb	41	59	68	44	39	42	40	45	57	63	47	0.05	39	68	50	45
Dy	216	357	419	270	207	209	222	212	346	355	254	0.25	207	419	279	254
Ho	42	63	75	50	38	36	47	40	66	66	48	0.06	36	75	52	48
Er	102	151	180	126	87	88	111	99	160	147	110	0.12	87	180	124	111
Tm	12	17	23	15	10	11	12	12	19	17	12	0.04	10	23	15	12
Yb	56	93	103	79	47	57	61	60	88	83	61	0.28	47	103	72	61
Lu	6.9	11	12	10	5.3	7.6	6.9	7.5	11	10	8.0	0.06	5.3	12	8.7	8.0
Sum REE	4951	8479	8236	6373	4064	5892	5125	5223	7723	8400	5821		4064	8479	6390	5892
Sum oxides (wt %)	106.42	106.27	96.68	103.98	100.33	95.77	91.68	101.84	101.86	102.83	105.09		91.68	106.42	101.16	101.86
Sr/Y	0.38	0.24	0.28	0.39	0.76	0.44	0.31	0.47	0.33	0.33	0.41		0.24	0.76	0.39	0.38
Ce/Ce*	1.00	0.99	1.00	1.01	0.99	1.05	1.03	0.97	1.02	0.99	1.00		0.97	1.05	1.01	1.00
Eu/Eu*	0.37	0.31	0.30	0.41	0.63	0.47	0.33	0.41	0.33	0.35	0.41		0.30	0.63	0.39	0.37
La <sub>N</sub> /Yb <sub>N</sub>	9.20	9.15	8.36	7.65	7.80	10.09	7.93	8.65	9.11	9.95	10.64		7.65	10.64	8.96	9.11
La <sub>N</sub> /Sm <sub>N</sub>	1.78	1.61	1.81	1.63	1.35	1.43	1.44	1.55	1.81	1.47	2.04		1.35	2.04	1.63	1.61
Gd <sub>N</sub> /Yb <sub>N</sub>	4.08	3.97	3.24	3.43	4.99	4.60	3.59	4.17	3.68	4.14	4.20		3.24	4.99	4.01	4.08
La/Sm	2.8	2.6	2.9	2.6	2.1	2.3	2.3	2.5	2.9	2.3	3.2		2.1	3.2	2.6	2.6
Y/REE	0.21	0.19	0.16	0.16	0.17	0.16	0.19	0.19	0.15	0.18	0.18		0.15	0.21	0.18	0.18
Ce/Th	115	131	118	151	110	143	155	152	143	140	202		110	202	142	143

concentrations of elements, which are usually not incorporated in apatite (such as Co, Cr, Ni, Sc, Sn, Ta and V) were either only slightly above or below the detection limit.

### 3.4.3. Zircon age-dating

For zircon dating and isotopic corrections with LA-ICP-MS, 3 natural zircon reference materials were used: FC1 (1099.0±0.6 Ma; PACES & MILLER, 1993), Peixe (564±4 Ma; DICKINSON & GEHRELS, 2003 and 558±2.7 Ma; SHAULIS et al., 2010), and Plešovice (337.13±0.37 Ma; SLÁMA et al., 2008). The following ions were measured:  $^{202}\text{Hg}$ ,  $^{204}(\text{Hg}+\text{Pb})$ ,  $^{206}\text{Pb}$ ,  $^{207}\text{Pb}$ ,  $^{208}\text{Pb}$ ,  $^{232}\text{Th}$ ,  $^{235}\text{U}$ ,  $^{238}\text{U}$ , and  $^{254/238}\text{U}^{16}\text{O}$ . The method and corrections used for data evaluation are described in detail in BALEN et al. (2020). By dating these 3 references as unknowns, using the aforementioned method and corrections, the obtained concordia ages plotted in a  $^{206}\text{Pb}/^{238}\text{U}$  vs.  $^{207}\text{Pb}/^{235}\text{U}$  diagram (FC1=1104.3±5.9 Ma, MSWD=0.5, n=8; Peixe=564.8±4.1 Ma, MSWD=0.2, n=6; Plešovice=335.6±3.7 Ma, MSWD=0.2, n=4) coincide with their literature values.

## 4. RESULTS

### 4.1. Outcrop and rock description

The Rupnica locality is a small abandoned quarry in the north-western part of Mt. Papuk within the Papuk Nature Park. It is a key geosite of the Papuk Geopark protected under the UNESCO supervision, and is well-known for its columnar jointing developed in albite rhyolite (Fig. 2a). The site is located near the town of Voćin (Fig. 1c, coordinates: 45.6049° N, 17.5320° E). BALEN & PETRINEC (2014) investigated the phenomenon of columnar jointing in detail, conducting a non-destructive statistical analysis of the geometric distribution of columns combined with petrography, geochemistry and the geology of the geosite. These authors suggested that the albite rhyolite formed via rapid cooling of a (sub)surface acidic lava body.

The albite rhyolite of the Rupnica locality and its variations (aegirine-albite and anorthoclase-aegirine rhyolite) are described as volcanic rocks, the chemical composition of which are not significantly affected by hydrothermal alteration or other types of

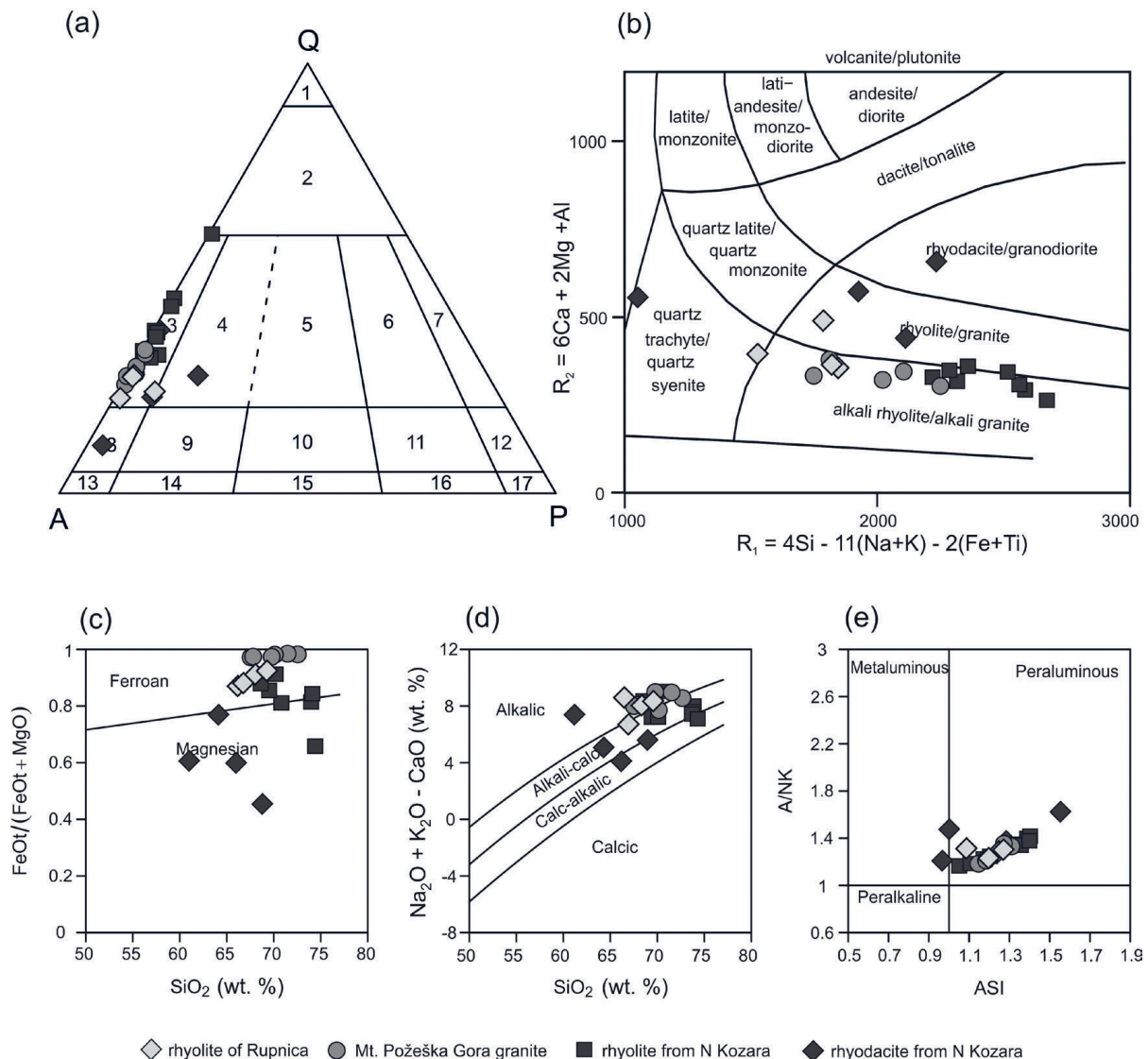


**Figure 3.** Comparison of the rhyolite of Rupnica, Mt. Požeška Gora granite and acidic effusive rocks from the northern part of Mt. Kozara: (a) QAP modal composition diagram after STRECKEISEN (1974, 1978) for both volcanic and plutonic rocks: Q – quartz; A – alkali feldspar; P – plagioclase; 2 – alkali-feldspar trachyte/Q-rich granite; 3 – alkali-feldspar rhyolite/alkali-feldspar granite; 4 – rhyolite/syenogranite; 8 – Q-alkali-feldspar trachyte/Q-alkali-feldspar syenite. Classification and discrimination diagrams based on major elements after (b) DE LA ROCHE et al. (1980), and (c–e) FROST et al. (2001) and FROST & FROST (2011). Geochemical data for the acidic effusive rocks from the northern part of Mt. Kozara are from USTASZEWSKI et al. (2009) and CVETKOVIĆ et al. (2014).

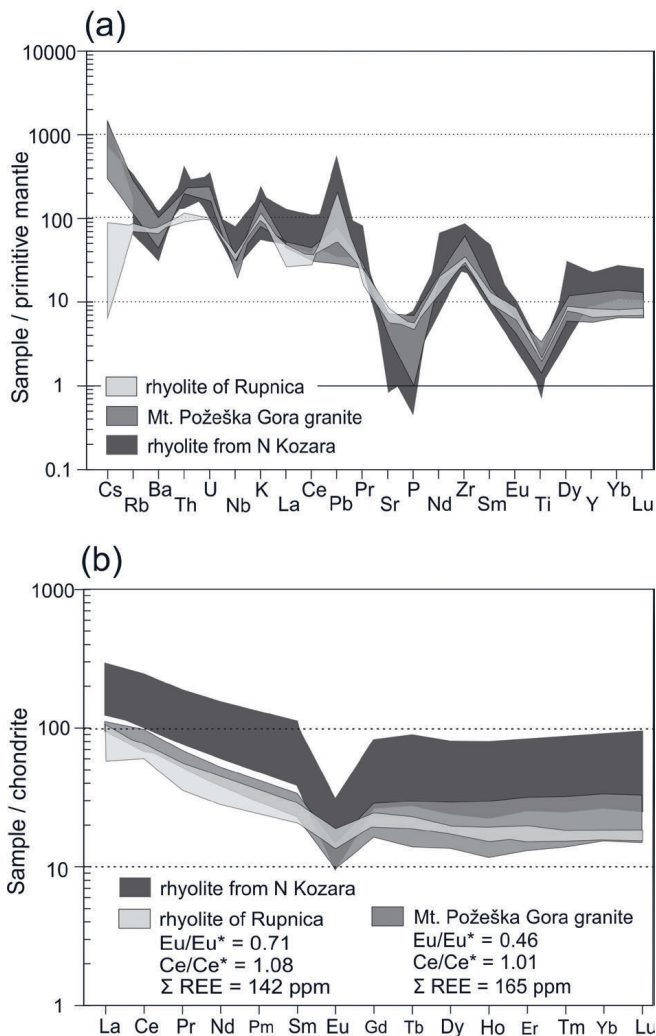


**Figure 4.** Comparison of the rhyolite of Rupnica, Mt. Požeška Gora granite and rhyolite from the northern part of Mt. Kozara: (a) primitive mantle whole-rock incompatible trace element patterns after SUN & MCDONOUGH (1989) and (b) whole-rock chondrite-normalized patterns of REE after BOYNTON (1984). References for Mt. Kozara are the same as in Fig. 3.

secondary processes (TAJDER, 1956, 1960). The rhyolites are leucocratic and light-grey to greenish in colour with porphyritic texture and phenocrysts of feldspar (albite). Detailed petrographic descriptions of albite rhyolite and its variations can be found in TAJDER (1956, 1960) and BALEN & PETRINEC (2014). Albite contains 98.1–99.9 % albite component (BALEN & PETRINEC, 2014) and occurs as phenocrysts (up to 30 vol. % of the rock) and as microliths in the fine-grained groundmass (Fig. 2b–c) together with a devitrified volcanic glass (up to 10 vol. %). Magnetite, apatite, zircon and in places alkali clinopyroxene (aegirine-augite) occur as accessory minerals, while kaolinite, illite, smectite, chlorite and calcite are secondary minerals. Haematite, apatite and anatase are found additionally as inclusions in zircon (see section 4.3.2. *Inclusions in zircon*).

#### 4.2. Whole-rock geochemistry

The rhyolite of Rupnica (Table 1, Fig. 3) is characterized by: (1) relatively high siliceous compositions ( $SiO_2$  up to 69.5 wt. %), (2) high abundance of alkalis ( $K_2O+Na_2O$  between 8.2 and 9.0 wt. % with  $K_2O$  up to 3.5 wt. %), (3) relatively high  $K_2O/Na_2O$  molar ratios (0.36–0.43), (4) high  $Al_2O_3$  (15.4–16.7 wt. %, molar A/CNK ratios =  $Al_2O_3/(CaO+Na_2O+K_2O)$  of 1.08–1.24, A/NK ratios =

$Al_2O_3/(Na_2O+K_2O)$  of 1.24–1.32), (5) low CaO (0.35–1.5 wt. %), MgO (0.27–0.53 wt. %), and MnO (<0.07 wt. %), and (6) relatively high  $Fe_2O_3$  contents (3.5–4.2 wt. %); thus, the  $FeO_T/(FeO_T+MgO)$  ratios (0.87–0.92) are high. These parameters indicate that the studied rocks are peraluminous, ferroan and alkali-calcic to alkalic (Fig. 3c–e).

In the primitive mantle-normalized element plot (Fig. 4a), the analysed rhyolite samples display positive anomalies of K, Pb, and Zr and relatively pronounced negative anomalies of P, Ba, Eu, Nb and Ti. Chondrite-normalized data of REE reveal an enrichment of light REE (LREE) relative to heavy REE (HREE) with  $(La/Yb)_N$ ,  $(La/Sm)_N$  and  $(Gd/Yb)_N$  of 3.47–5.92, 2.76–3.64, and 1.20–1.40, respectively (Fig. 4b).  $Eu/Eu^*$  parameters are between 0.66 and 0.74, whereas  $Ce/Ce^*$  ranges between 0.96 and 1.33. The sum of REE is around 142 ppm. Contents of Y and Yb are around 32 ppm and 3.5 ppm, respectively. The data presented for the major elements are in the good agreement with previous data from TAJDER (1956, 1960) and PAMIĆ (1991) for rhyolite of Rupnica.

#### 4.3. Accessory minerals analyses

##### 4.3.1. Zircon external morphology

The population of zircon analysed for external morphology consists of 65 grains which are 50–110  $\mu m$  long and 25–55  $\mu m$  wide. Aspect ratios range from 1.4:1 to 3.3:1, with the median value of 2.3:1. Such ratios, the colourlessness, high transparency and birefringence are usually characteristic of early crystallized zircon in a granitic magma (HOSKIN & SCHALTEGGER, 2003). Around 40 % of the examined zircon population is partially dissolved, so the external morphology could not always be clearly defined. The rest of the separated zircon, i.e. grains with recognizable external morphology, was carefully examined. Their external morphology is defined by {100} prisms and {101} > {211} bipyramids. After PUPIN's (1980) zircon typology, types J4 (50 %), J3 (30 %), J5 (10 %) and J2 (<10 %) are present (Fig. 5). According to PUPIN & TURCO (1972) and PUPIN (1980), such morphologies are considered to characterize zircon crystallized from high-temperature magmas with lower crust or upper mantle origin.

##### 4.3.2. Inclusions in zircon

Zircon grains are very rich in inclusions. Even dozens of them can occur in a single zircon grain and therefore represent potential material for further detail research. The inclusions vary in shape; some of them are euhedral and needle-like, but all are smaller than 10  $\mu m$ . Raman bands of zircon (at 202, 212, 225, 356, 392, 438, 972–974 and 1005–1008  $cm^{-1}$ , strongest at 356, 972–974 and 1005–1008  $cm^{-1}$ , after FREZZOTTI et al., 2012), despite the confocal mode, are very intense, making the identification of included phases difficult. So far, inclusions of haematite (bands at 223, 290, 409, 498, 609 and 1313  $cm^{-1}$ , strongest at 290 and 409  $cm^{-1}$ , after FREZZOTTI et al., 2012), apatite (bands at 432, 449, 581, 592, 608, 965, 1042, 1053 and 1081  $cm^{-1}$ , strongest at 965  $cm^{-1}$ ; characteristic for F-apatite after HURAI et al., 2015; bands at 3100–3800  $cm^{-1}$  characteristic for O-H were not detected) and anatase (143, 195, 395, 514 and 638  $cm^{-1}$ , strongest at 143 and 638  $cm^{-1}$ , after FREZZOTTI et al., 2012) were detected (Fig. 6).

##### 4.3.3. Zircon geochemistry

For zircon geochemistry, 14 grains were successfully analysed with LA-ICP-MS. The results, together with basic statistical parameters and characteristic elemental ratios, are presented in Table 2. Zircon from the rhyolite of Rupnica shows variable

U (137–958, mean 443 ppm) and Th (107–1411, mean 531 ppm) contents, with Th/U ratios between 0.78 and 1.62 (mean 1.13), typical for igneous zircon (HOSKIN & SCHALTEGGER, 2003; KIRKLAND et al., 2015).

The compositional range of the determined REE patterns (Fig. 7a) is characteristic for zircon from granitoids (BELOUSOVA et al., 2002a; HOSKIN & SCHALTEGGER, 2003) with significant rise of contents from Sm to Lu and total contents of REE between 1155 and 4490 ppm (mean 2993 ppm). A positive Ce anomaly (mean 1.27) indicates oxidized magma conditions, as does the finding of haematite as a primary inclusion in zircon.

#### 4.3.4. Zircon U-Th-Pb dating

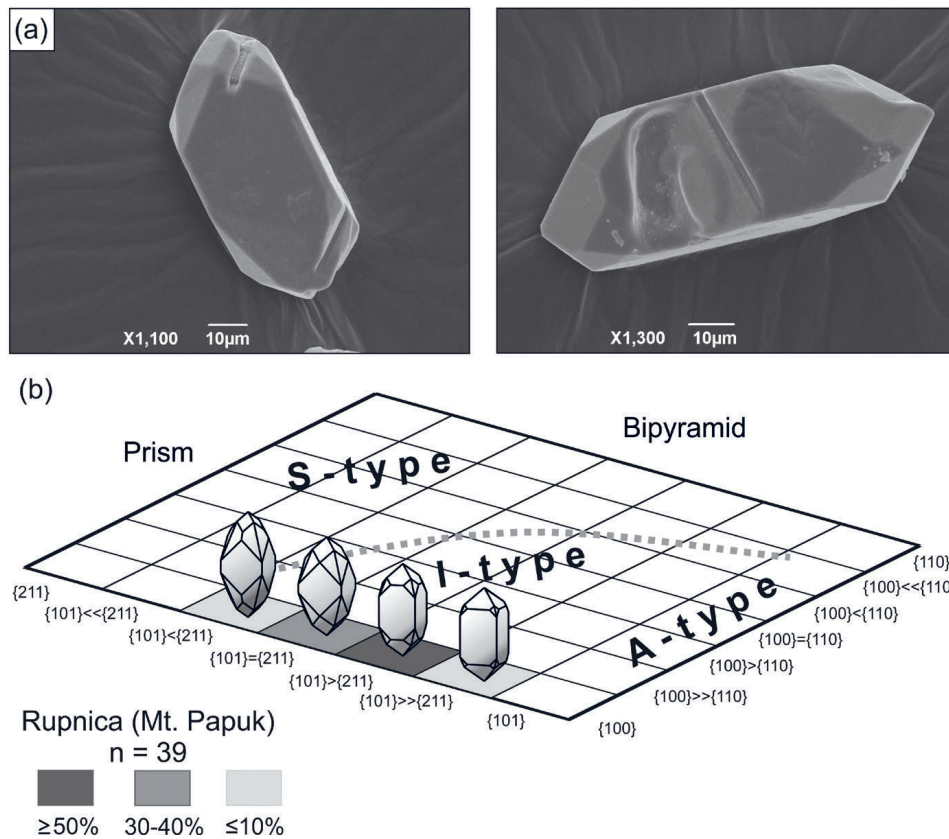
The results of dating on 20 zircon grains from the Rupnica locality, selected on the basis of euhedral shape and elemental ratios (such as Th/U), are presented in Table 4 and in a concordia diagram in Fig. 8. Zircon yielded a concordia age of  $80.8 \pm 1.8$  ( $2\sigma$ ) Ma and a mean square weighted deviation (MSWD) of 0.8. The zircon ages determined from the individual calibrated quotients of isotopic intensities  $^{206}\text{Pb}/^{238}\text{U}$ ,  $^{207}\text{Pb}/^{235}\text{U}$  and  $^{208}\text{Pb}/^{232}\text{Th}$  are  $80.0 \pm 2.1$ ,  $82.7 \pm 3.3$  and  $81.7 \pm 1.8$  Ma, respectively, with errors given as  $2\sigma$  values. The MSWD values of 0.76, 0.45 and 1.00, respectively, suggest a single zircon generation.

**Table 4.** Individual elemental and isotopic concentrations and ages of zircon from the rhyolite of Rupnica obtained from calibrated isotopic ratios of  $^{206}\text{Pb}/^{238}\text{U}$ ,  $^{207}\text{Pb}/^{235}\text{U}$ , and  $^{208}\text{Pb}/^{232}\text{Th}$ . Elemental concentrations of Pb refer to the sum of the Pb isotopes.

Grain	Elemental concentrations						Isotopic concentrations (ppm)			
	Si (wt. %)	Zr (wt. %)	Th (ppm)	U (ppm)	Pb (ppm)	Th/U	$^{204}\text{Pb}$	$^{206}\text{Pb}$	$^{207}\text{Pb}$	$^{208}\text{Pb}$
1b	15.14000	47.13930	495.67	492.20	7.64	1.01	0.004	5.13	0.36	2.14
2b	15.14000	42.77307	328.12	343.58	7.41	0.96	0.024	4.39	0.60	2.40
3b	15.14000	46.23996	785.15	667.36	12.81	1.18	0.034	8.07	0.78	3.93
4b	15.14000	44.05930	221.57	279.74	4.89	0.79	0.052	3.28	0.30	1.26
5b	15.14000	43.30943	825.65	696.89	14.78	1.18	0.033	8.75	1.11	4.89
6b	15.14000	44.56110	404.35	517.83	9.19	0.78	0.013	6.50	0.55	2.12
7b	15.14000	43.86399	444.66	443.50	8.04	1.00	0.005	5.56	0.41	2.05
8b	15.14000	47.62453	770.86	705.22	13.30	1.09	0.001	9.00	0.66	3.65
9b	15.14000	48.44948	1552.14	917.59	18.77	1.69	0.012	12.21	0.70	5.85
10b	15.14000	45.80696	525.60	493.64	8.70	1.06	0.000	5.98	0.44	2.28
11b	15.14000	45.34541	828.67	684.20	11.90	1.21	0.017	8.40	0.41	3.08
12b	15.14000	44.69870	785.57	659.58	14.01	1.19	0.018	9.02	0.90	4.07
13b	15.14000	50.44010	524.08	476.65	10.30	1.10	0.058	6.30	0.79	3.15
14b	15.14000	48.10264	458.37	448.63	7.66	1.02	0.022	5.11	0.44	2.09
15b	15.14000	48.20173	964.95	718.38	13.46	1.34	0.023	8.23	0.82	4.38
16b	15.14000	43.88730	2157.05	1263.47	24.03	1.71	0.010	15.30	0.83	7.88
17b	15.14000	49.07538	386.88	281.20	5.82	1.38	0.026	3.62	0.34	1.83
18b	15.14000	49.54529	933.63	691.47	14.00	1.35	0.014	8.30	0.80	4.89
19b	15.14000	49.07977	396.54	360.44	7.04	1.10	0.016	4.73	0.42	1.87
20b	15.14000	48.50643	419.63	426.19	7.52	0.98	0.019	5.01	0.38	2.12

Grain	Isotopic ratios						Age (Ma)					
	$^{206}\text{Pb}/^{238}\text{U}$	$1\sigma$	$^{207}\text{Pb}/^{235}\text{U}$	$1\sigma$	$^{208}\text{Pb}/^{232}\text{Th}$	$1\sigma$	$^{206}\text{Pb}/^{238}\text{U}$	$1\sigma$	$^{207}\text{Pb}/^{235}\text{U}$	$1\sigma$	$^{208}\text{Pb}/^{232}\text{Th}$	$1\sigma$
1b	0.01160	0.00061	0.07659	0.00536	0.00421	0.00018	74.3	3.9	74.9	5.1	85.1	3.6
2b	0.01214	0.00063	0.08326	0.02146	0.00449	0.00066	77.8	4.0	81.2	20.1	90.9	13.3
3b	0.01228	0.00069	0.08622	0.01491	0.00410	0.00019	78.7	4.4	84.0	13.9	82.8	3.9
4b	0.01185	0.00041	0.07631	0.01193	0.00433	0.00041	75.9	2.6	74.7	11.3	87.6	8.3
5b	0.01221	0.00100	0.08209	0.01861	0.00412	0.00027	78.2	6.4	80.1	17.5	83.3	5.4
6b	0.01287	0.00132	0.08643	0.01170	0.00404	0.00018	82.4	8.4	84.2	10.9	81.7	3.6
7b	0.01310	0.00088	0.08697	0.00913	0.00407	0.00019	83.9	5.6	84.7	8.5	82.3	3.9
8b	0.01296	0.00087	0.09118	0.01000	0.00429	0.00012	83.0	5.6	88.6	9.3	86.7	2.5
9b	0.01383	0.00095	0.09191	0.00627	0.00385	0.00011	88.6	6.1	89.3	5.8	78.0	2.3
10b	0.01243	0.00042	0.08519	0.00735	0.00385	0.00020	79.6	2.7	83.0	6.9	77.8	4.1
11b	0.01319	0.00081	0.08792	0.00330	0.00397	0.00023	84.5	5.1	85.6	3.1	80.4	4.7
12b	0.01366	0.00109	0.09348	0.02380	0.00399	0.00054	87.5	6.9	90.7	22.1	80.7	10.9
13b	0.01332	0.00086	0.08398	0.01203	0.00393	0.00020	85.3	5.5	81.9	11.3	79.5	4.0
14b	0.01147	0.00124	0.07905	0.01466	0.00373	0.00028	73.5	7.9	77.3	13.8	75.6	5.7
15b	0.01178	0.00182	0.07547	0.01261	0.00368	0.00026	75.5	11.6	73.9	11.9	74.4	5.2
16b	0.01294	0.00101	0.08967	0.00631	0.00390	0.00017	82.9	6.4	87.2	5.9	78.9	3.4
17b	0.01322	0.00092	0.08653	0.01349	0.00392	0.00023	84.7	5.9	84.3	12.6	79.2	4.6
18b	0.01277	0.00073	0.08081	0.00622	0.00434	0.00015	81.8	4.6	78.9	5.8	87.7	3.1
19b	0.01351	0.00071	0.08925	0.01587	0.00372	0.00027	86.5	4.5	86.8	14.8	75.3	5.4
20b	0.01192	0.00069	0.07766	0.00590	0.00420	0.00024	76.4	4.4	75.9	5.6	84.9	4.9
Weighted average (Ma)							80.0		82.7		81.7	
Error $2\sigma$ (Ma)							2.1		3.3		1.8	
MSWD							0.76		0.45		1.00	



**Figure 5.** (a) Typical external morphologies of zircon from the rhyolite of Rupnica. (b) Morphologies and types of investigated zircon grains shown on the modified zircon typology diagram after PUPIN (1980).

#### 4.3.5. Apatite geochemistry

For apatite geochemistry, 11 grains were successfully analysed with LA-ICP-MS (Table 3). REE patterns (Fig. 7b) with total contents of REE between 4064 and 8479 ppm (mean 6390 ppm) display a negative slope according to the relative enrichment of the LREE, with a  $(La/Yb)_N$  mean ratio of 9.0, which is typical for apatite from granitoids (BELOUSOVA et al., 2002b). Pronounced negative Eu anomalies with a mean of 0.39 were determined. This mean is close to the average for apatite from granitoid rock types (BELOUSOVA et al., 2002b).

#### 4.4. Geothermometry

A zircon saturation temperature (ZST) was calculated after WATSON & HARRISON (1983) and GERVASONI et al. (2016), using whole-rock Zr concentrations (Table 1). A negative  $SiO_2$ -Zr covariation occurs in the whole-rock data for the rhyolite of Rupnica. Therefore,  $ZrSiO_4$  saturation during early magmatic crystallization is assumed (SCHILLER & FINGER, 2019). Calculated temperatures are within a narrow range of 858–867 °C (mean 863 °C) using parameters from WATSON & HARRISON (1983), indicating a high-temperature environment. Calculations with the model by GERVASONI et al. (2016), which is considered to give more reliable values, yielded lower temperatures of 778–798 °C (mean 789 °C), but these would still correspond to a high-temperature environment.

The Ti-in-zircon temperature after WATSON et al. (2006) was calculated for selected grains that are characterized by relatively low Ti contents, i.e. analyses that exclude Ti-rich inclusions (Table 2). Calculated temperatures are 801–831 °C (mean 814 °C) with a precision of  $\pm 5$  °C (WATSON et al., 2006). These temperatures fit the range of the calculated ZST and are only slightly

lower than the ZST after WATSON & HARRISON (1983). Such a temperature difference is common for samples with  $M$  (cation ratio) =  $(Na+K+2Ca)/Al-Si < 1.9$  (FU et al., 2008; Fig. 9).

The apatite saturation temperature (AST) calculated after HARRISON & WATSON (1984) for metaluminous to slightly peraluminous systems is 900 °C. As apatite generally crystallizes over a relatively restricted interval within 60–100 °C of the AST (PICCOLI & CANDELA, 1994, 2002), the calculated AST would imply crystallization of apatite prior to crystallization of zircon (corroborated by apatite inclusions in zircon) or during zircon crystallization. Because ZST and AST are based on the whole-rock analysis and not on glass separates, the calculated temperatures are considered to represent maximum ones (KIRKLAND et al., 2015).

## 5. DISCUSSION

### 5.1. Whole-rock geochemistry and comparison with an A-type granite at Mt. Požeška Gora

The whole-rock geochemistry in this paper was intended to provide the geochemical environment for zircon and apatite crystallization in the studied rocks. However, whole-rock geochemistry presented here shows noticeable similarities with the A-type granite of Mt. Požeška Gora, despite the limited number of analysed samples.

PAMIĆ (1997) associated the Voćin volcanic rocks with those at Mt. Požeška Gora. It was assumed that (sub-)volcanic rocks from both localities have a similar age and are therefore associated to a unique Senonian basalt-rhyolite formation, although the volcanic rocks at Mt. Požeška Gora also comprise A-type granite. PAMIĆ (1997) suggested a connection of these masses

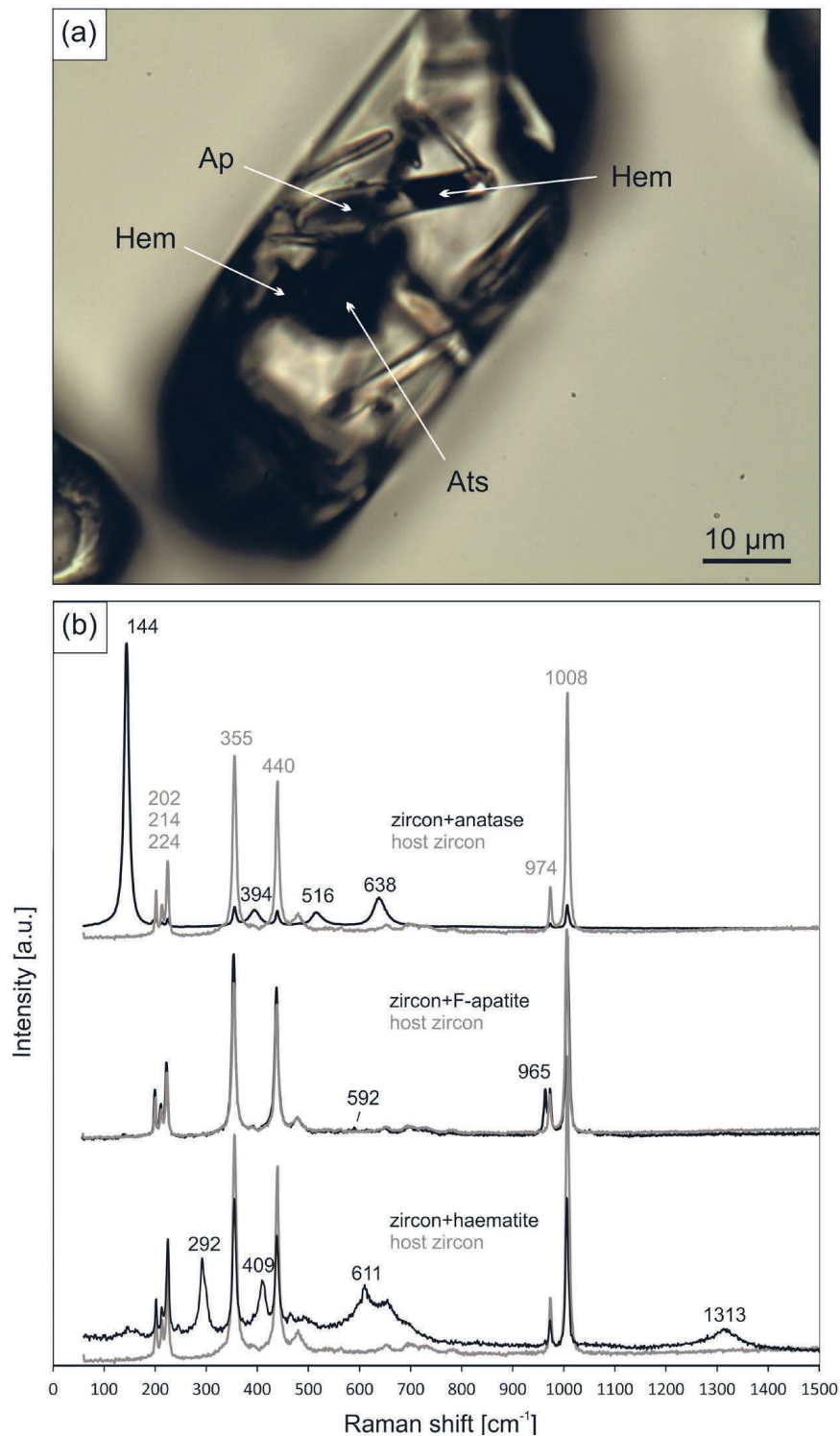


**Figure 6.** (a) Plain-polarized transmitted-light photomicrograph of a zircon grain rich in inclusions. Arrows indicate the analytical spots for Raman spectrometry and detected inclusions. Magnification 1000x. Ap – apatite; Ats – anatase; Hem – haematite. (b) Raman spectra of anatase, apatite and haematite inclusions in zircon. Spectra were compared with data given by FREZZOTTI et al. (2012) and HURAI et al. (2015).

and a Late Cretaceous age based on petrography, geochemistry and mineralogical features of the samples. In addition, the rather arguable age data of K-Ar dating on basalts from Voćin (72.8–51.7 Ma; PAMIĆ, 1991) and the application of the Rb-Sr isochron method to granite and rhyolite from Mt. Požeška Gora (71.5±2.8 Ma; PAMIĆ et al., 1988) were used to support this connection. The latter age was recently revised by LA-ICP-MS dating of zircon to 83.6±1.5 Ma by BALEN et al. (2020). The zircon age fits geological relations to the surrounding sedimentary rocks.

When comparing mean values of whole-rock major element contents of granite from Mt. Požeška Gora (BALEN et al., 2020, PAMIĆ, 1987) and rhyolite of Rupnica (Table 1), the following similar mean values were found: (1) highly siliceous compositions (69.9 and 67.75 wt. % SiO<sub>2</sub>, respectively); (2) enrichment in alkalis (K<sub>2</sub>O+Na<sub>2</sub>O content: 8.68 and 8.60 wt. %); (3) relatively high K<sub>2</sub>O/Na<sub>2</sub>O molar ratios (0.56 and 0.40); (4) high Al<sub>2</sub>O<sub>3</sub> contents (15.3 and 15.8 wt. % Al<sub>2</sub>O<sub>3</sub>; A/CNK ratio = 1.21 and 1.19; A/NK ratio = 1.27 and 1.28); (5) low contents of CaO (0.28 and

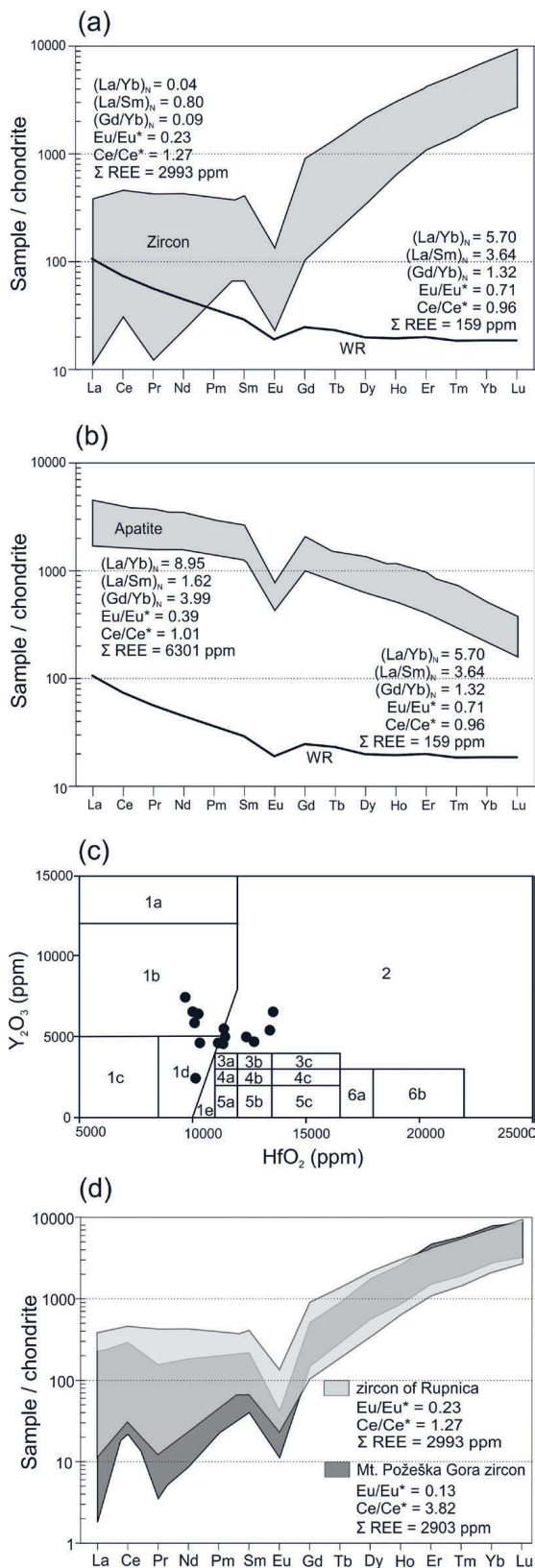


**Figure 7.** (a) Chondrite-normalized patterns of REE in (a) zircon and (b) apatite grains separated from the rhyolite of Rupnica using normalizing factors after BOYNTON (1984). Result of the whole-rock (WR) analysis of sample Rupnica 3, from which zircon and apatite grains were separated (thick line), is given for comparison. (c) HfO<sub>2</sub> versus Y<sub>2</sub>O<sub>3</sub> diagram after PUPIN (2000). Fields 1–2 are specific domains for anorogenic rocks, fields 5–6: orogenic rocks, fields 3–4 both types of rocks. 1b – hypersolvus alkaline granite/rhyolite; 1d – hypersolvus alkaline granite/rhyolite or silica over/under-saturated alkaline/peralkaline syenite/trachyte; 2 – subsolvus alkaline granite/rhyolite. For other fields see the reference. (d) Chondrite-normalized patterns of REE after BOYNTON (1984); comparison of zircon grains from Mt. Požeška Gora granite and the rhyolite of Rupnica.

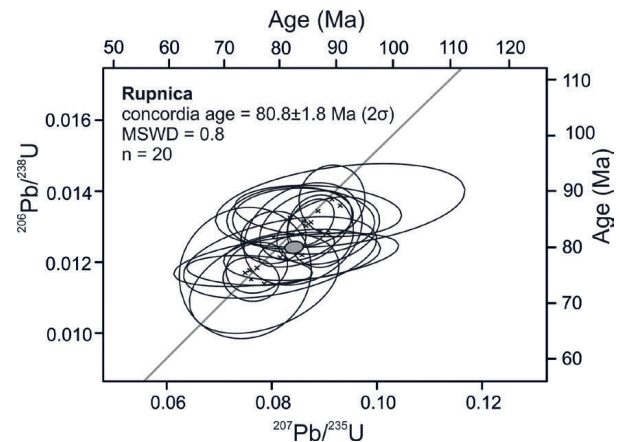


**Figure 8.** U-Pb concordia diagram for zircon from the rhyolite of Rupnica. Error ellipses relate to 1σ errors. Weighted average ages, errors and MSWD values are given in Table 4.

0.64 wt. %), MgO (0.07 and 0.42 wt. %), and MnO (<0.08 wt. %); (6) relatively high Fe<sub>2</sub>O<sub>3</sub> contents (3.30 and 3.84 wt. %); (7) high FeO<sub>T</sub>/(FeO<sub>T</sub>+MgO) ratios (0.98 and 0.89). According to the listed parameters, both the Mt. Požeška Gora granite and the rhyolite of Rupnica refer to peraluminous, oxidized, ferroan, and alkali-calcic to alkalic magmas (Fig. 3c–e).

Trace element contents in both the granite from Mt. Požeška Gora (BALEN et al., 2020) and the rhyolite of Rupnica are also similar (Fig. 4). In the primitive mantle-normalized element plots (Fig. 4a) both rock types display positive anomalies of K, Pb, and Zr and relatively pronounced negative anomalies of high field strength elements (HFSE), P, Ba and Eu. The main differences concern the contents of Cs, U and Th. Whole-rock Zr/Hf ratios are also similar (mean: 39 for granite and 42 for rhyolite) and fall in the range for the average continental crust (PUPIN, 2000). Chondrite-normalized data of REE (Fig. 4b) reveal an enrichment of LREE relative to HREE with pronounced negative Eu anomalies (mean: 0.46 for granite and 0.71 for rhyolite) and minor positive Ce anomalies (mean: 1.01 for granite and 1.08 for rhyolite). The mean sum of REE is 165 ppm for the granite and 142 ppm for the rhyolite.

REE patterns of the rhyolite of Rupnica do not show the tetrad effect implying the absence of a significant H<sub>2</sub>O content in the melt (MCLENNAN, 1994). Instead, according to the Zr/Hf (39–43) and Y/Ho (25–28) ratios, the element distribution is CHARAC (CHARGE and RADIUS CONTROLLED, BAU, 1996). Pat-

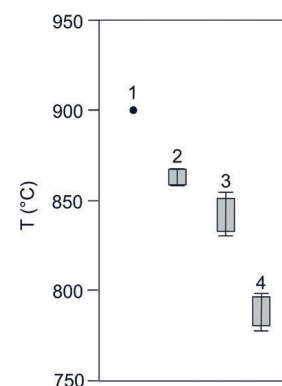


**Figure 9.** Boxplot of temperature ranges for different geothermometers: 1 – apatite saturation temperature (AST) after HARRISON & WATSON (1984); 2 – zircon saturation temperature (ZST) after WATSON & HARRISON (1983); 3 – Ti-in-zircon after WATSON et al. (2006); 4 – ZST after GERVASONI et al. (2016).

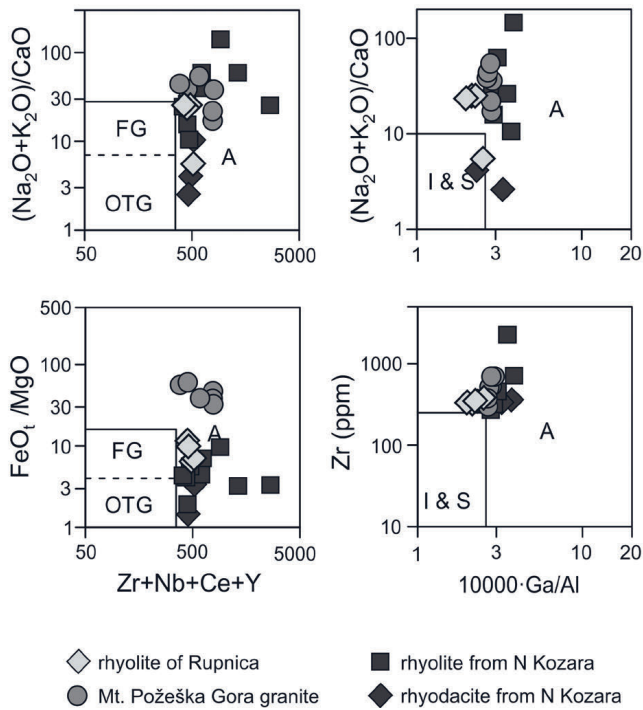


**Figure 10.** Diagrams to discriminate A-type granitoids after WHALEN et al. (1987). I, S, and A denote I-, S-, and A-type granites, respectively. FG – fractionated felsic granites; OTG – unfractionated M-, I-, and S-type granites.

terns of incompatible trace elements (Fig. 4a and 4b), trace element ratios (Table 1), apparent enrichments in LREE together with intermediate-to-low contents of HFSE (except Hf and Zr), variable abundances of large ion lithophile elements (LILE), and negative Eu anomalies (Fig. 4b) point to crustal sources of the corresponding magmas.

According to the geochemistry in respect to reference materials (BOYNTON 1984; SUN & MCDONOUGH, 1989), standard geotectonic classification diagrams and classification of granitic rocks by WHALEN et al. (1987), EBY (1990, 1992) and KING et al. (1997), the rhyolite of Rupnica shows A-type features (Figs. 10 and 11), which are relatively high contents of HFSE (Ga, Nb, Ta, Th, U, Y, Zr); significantly enriched LILE compared to primitive mantle, high FeO\* (>1 wt. %), K and total contents of REE, 10000 · Ga/Al ratios of 2.0–2.5, and low MgO, CaO, Cr, Ni, Sr and Ba contents.

Furthermore, the temperature characteristics for magmas forming the albite rhyolite of Rupnica and the granite of Mt. Požeška Gora are similar. Both rocks originated from hot (ca. 800–900 °C), dry and oxidized magmas generated at lower- to mid-crustal levels. An inhomogeneous source at such depth can be expected (KEMPTON et al., 1990; BUROV et al. 2007), where tonalitic to granodioritic crust produces peraluminous alkali-calcic to calc-alkalic granitic melts (PATIŃO DOUCE 1997; FROST & FROST, 2011) by a low degree of partial melting at higher pressures (see SKJERLIE & JOHNSTON, 1993, for magnesian tonalite at pressures ≥ 10 kbar). A relatively fast ascent to (sub)surface levels of the A-type magma led to rhyolite with glass in the matrix at Rupnica.

**5.2. Chemical compositions of zircon and apatite and their petrogenetic significance**

Normalized patterns of REE in zircon, not contaminated by inclusions, demonstrate the igneous nature by negative Eu anomalies and enrichment of HREE (Fig. 7a) with generally high sums

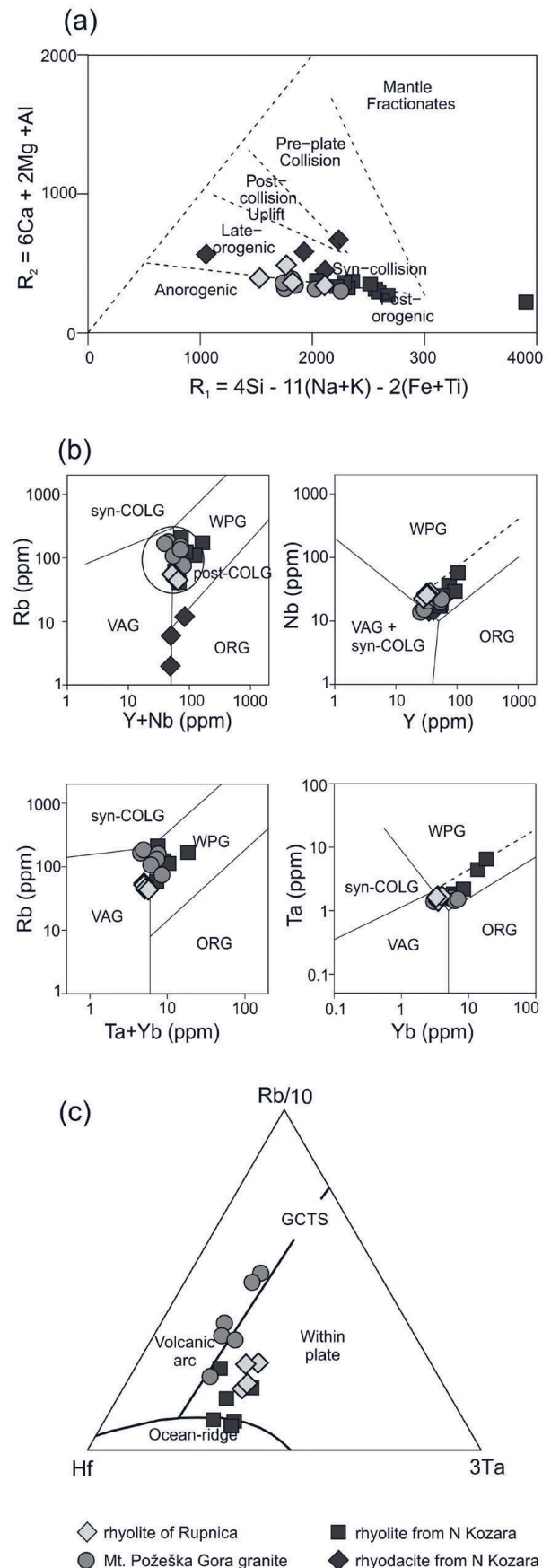


**Figure 11.** (a) Geotectonic discrimination diagram after BATCHELOR & BOWDEN (1985), (b) geotectonic discrimination diagrams for granites after PEARCE et al. (1984) and PEARCE (1996) and (c) after HARRIS et al. (1986). VAG – volcanic arc granites, WPG – within-plate granites, syn-COLG – syn-collision granites, ORG – ocean-ridge granites, post-COLG – post-collision granites, GCTS – granites from collisional tectonic setting.

of REE. The positive Ce and significantly negative Eu anomalies are typical for zircon from granitoids especially for those with 65–70 wt. % of SiO<sub>2</sub> (BELOUSOVA et al., 2002a). A less developed Eu anomaly accompanied by an enhanced Hf content in zircon indicates co-crystallization of zircon and plagioclase (SŁODCZYK et al., 2016). Relative enrichment in HREE over medium REE and apatite and a Ti-phase detected by Raman spectroscopy as inclusions in zircon suggest the co-crystallization of these phases (HOSKIN et al., 2000). In the Rupnica samples, apatite also occurs as individual grains, which combined with AST values point to early crystallization of the apatite prior to or simultaneous with zircon.

Chemical compositions of zircon (e.g. Hf, Th, U) define it as an early crystallized mineral formed in a deep magma chamber at relatively high and constant temperatures (WANG et al., 2010; KIRKLAND et al., 2015). According to WANG et al. (2010), an early-stage zircon is characterized by high Zr/Hf ratios (~39; compared to late-stage zircon ~29) and low Hf concentrations (~1.35 wt. % HfO<sub>2</sub> compared to 1.85 wt. % for the late-stage), which fit the chemistry of the studied zircon (mean Zr/Hf=55, HfO<sub>2</sub>=1.04 wt. %).

Zircon of Rupnica has Hf concentrations of 6436–11511 ppm (mean 8784 ppm), which are characteristic of highly-evolved magmas (BELOUSOVA et al., 2002a). According to PUPIN (2000), whole-rock and zircon Zr/Hf ratios are indicative of magmatic fractionation of a granitic melt. A decrease of these ratios in zircon from mantle-derived plagiogranites (median 60–70), through hypersolvus alkali granites, alkali syenites and hybrid calc-alkaline granitoids to the lowest values in peraluminous granites and migmatites (median 35–37) was noted by PUPIN (2000). In other words, the higher this ratio the higher is the mantle input in the generated magma. For the studied zircon, the Zr/Hf ratio is on average 55, which points to a chemical mantle contribution to the magma. This view is supported by BALEN et al. (2020) who suggested a potential influence from a mantle source on the magma forming the A-type granite of Mt. Požeška Gora based on Zr/Hf ratio, morphology of zircon and inclusions therein. Furthermore, the Zr/Hf ratio of zircon crystallizing from a water-undersaturated melt is higher than the whole-rock Zr/Hf ratio (ERDMANN et al., 2013; BREITER & ŠKODA, 2017), which is valid for the rhyolite of Rupnica (mean whole-rock Zr/Hf ratio = 42).

Zircon grains extracted from the Mt. Požeška Gora granite and the rhyolite of Rupnica also show similar geochemical signatures (Fig. 7d) with mean zircon Zr/Hf ratios of 55 and 53, respectively, and Th/U ratios of 0.74 and 1.13, respectively. These signatures point to a magma origin by partial melting of material from mid- to lower-crustal levels (HOSKIN & SCHALTEGGER, 2003).

The high-temperature environment determined here by ZST, Ti-in-zircon and AST (789–863, 814 and 900 °C, respectively) was also found for the early crystallization of the studied accessory minerals in the Mt. Požeška Gora granite (BALEN et al., 2020) with ZST of 830–950 °C (mean 873 °C). Furthermore, zircon morphologies after PUPIN (1980) with D and J5 type prevailing in Mt. Požeška Gora granite and J4 and J3 in the rhyolite of Rupnica also suggest a high-temperature environment which is typical for an I- and/or an A-type granitic melt. Zircon crystallized from a magma which originated in the lower crust, but contributions from an upper mantle source should not be excluded due to the external zircon morphology (PUPIN & TURCO, 1972; PUPIN, 1980) and zircon Zr/Hf ratios (PUPIN, 2000). This crystallization occurred in a deep magma chamber at relatively con-

stant temperature > 800 °C (WANG et al., 2010; KIRKLAND et al., 2015).

The amplitude of Eu anomalies in apatite generally increases toward more fractionated rocks and is controlled by the crystallization of feldspar (BELOUSOVA et al., 2002b). Contents of Mn are expected to be relatively high in apatite crystallized from a magma under reduced conditions (BELOUSOVA et al., 2002b, reported Mn contents of 0.1–1 wt. %). Moreover, BELOUSOVA et al. (2002b) demonstrated that there is an excellent correlation between contents of REE in apatite and the oxidation state of the magma. Apatite from more oxidized granitic melts shows lower Y/ΣREE and higher La/Sm and Ce/Th ratios than apatite from less oxidized rocks, regardless of the overall degree of fractionation of the magma. Following such relations, the apatite from Rupnica with Y/ΣREE=0.18, La/Sm=2.6 and Ce/Th=142 crystallized in an oxidizing environment. This environment is also confirmed by primary inclusions of haematite in zircon from the rhyolite of Rupnica and the red granite from Mt. Požeška Gora (BALEN et al., 2020).

### 5.3. Implications on the regional setting

Considering the afore-mentioned characteristics of the whole rock and the accessory minerals therein, it can be assumed that the magmas forming the Mt. Požeška Gora granite and the rhyolite of Rupnica have the same origin. Thus, the rhyolite of Rupnica should be considered as a part of an igneous suite that intruded not only the Sava Zone, but also the adjacent Tisia Mega-Unit. This also concerns the Mt. Požeška Gora granite together with the Mt. Prosara leucogranite (82.68±0.13 Ma; PAMIĆ & INJUK, 1988; PAMIĆ & LANPHERE, 1991b; USTASZEWSKI et al., 2009) and Late Cretaceous acidic rocks from Mt. Moslavačka Gora (82±1 Ma; STARJAJŠ et al., 2010; BALEN & BROSKA, 2011; BALEN & PETRINEC, 2011), but also basic rocks from the latter locality which show upper mantle isotopic signatures (109±8 and 83±9 Ma; BALEN et al., 2003). Also rhyolites from the northern part of Mt. Kozara (USTASZEWSKI et al., 2009; CVETKOVIĆ et al., 2014), located in northern Bosnia and Herzegovina south of the Slavonian Mts. (Figs. 1 and 3), can be included in the comparison. These rhyolites with a mean zircon <sup>206</sup>Pb/<sup>238</sup>U age of 81.60±0.12 Ma (USTASZEWSKI et al., 2009) are part of a bimodal magmatic association. Mafic rocks of the same age occur and, according to geochemistry (normalized patterns of REE), originated from the same magma source as the acidic rocks. USTASZEWSKI et al. (2009) placed these rocks into an intra-oceanic environment (island-arc, ocean island or mid-ocean ridge setting), based on Sr and Nd isotopes.

CVETKOVIĆ et al. (2014) focused more on the acidic rocks of the bimodal association from the northern part of Mt. Kozara and confirmed the close petrogenetic link between basic and acidic rocks. Furthermore, these authors revisited the basic suite and concluded that the entire ophiolite slice from the northern part of Mt. Kozara could represent the remnant of an anomalous ridge segment (similar to present day Iceland). Cogenetic acidic magmas most probably originated through the obduction-induced partial melting of hydrated oceanic crust. These voluminous magmas were emplaced as subaerial high-temperature rhyodacite-rhyolite.

Discrimination diagrams after BATCHELOR & BOWDEN (1985) place rhyolites from the northern part of Mt. Kozara together with the rhyolite of Rupnica and the Mt. Požeška Gora granite in an anorogenic or postorogenic environment, whereas rhyodacites from Mt. Kozara point to a somewhat different environment (Fig. 11a). Rhyolite of Rupnica and the Mt. Požeška

Gora granite plot into the within plate or, less clearly, into the volcanic arc field (Fig. 11b) of the discrimination diagrams after PEARCE et al. (1984), whereas the rhyolite of Rupnica can be discriminated from the Mt. Požeška Gora granite (within-plate setting vs. volcanic arc setting, Fig. 11c) in the Rb-Hf-Ta diagram by HARRIS et al. (1986). According to HfO<sub>2</sub> vs. Y<sub>2</sub>O<sub>3</sub> contents (7590–13574 ppm HfO<sub>2</sub>, mean 10372 ppm; 1495–7815 ppm Y<sub>2</sub>O<sub>3</sub>, mean 5033 ppm), which are directly connected to the contrasting Hf and Y contents in zircon of orogenic and anorogenic rocks (PUPIN, 2000), zircon from the rhyolite of Rupnica crystallized from a hypersolvus or subsolvus alkaline granitic magma of anorogenic origin (Fig. 7c).

According to the data presented here and those by BALEN et al. (2020) discussed above, the rhyolite of Rupnica with a zircon U-Pb age of 81 Ma is related to the magmatism within the Sava Zone, i.e. the collisional environment between the Adria and Tisia microplates, and in the adjacent Tisia Mega-Unit. This collision with Adria as a subducted plate caused hot mantle to rise, leading to local extensional rift processes in the suture zone. The subsequent crustal extension caused a fast extrusion of rhyolitic magmas to the (sub)surface.

The igneous rocks of the Banatitic Magmatic and Metallogenic Belt (BMMB, BERZA et al., 1998) of Late Cretaceous age (ZIMMERMAN et al., 2008; overview in ILINCA et al., 2011), known as *banatites*, extend to the Balkan-South Carpathian orogenic belt in southeastern Europe. Although the petrology of the *banatites* is extremely diverse, geochemical data (trace elements and isotope composition) point to subduction related magmas with sources in the upper mantle or even lower crust (ILINCA et al., 2011). For the formation of the BMMB a slab rollback model is plausible (ZIMMERMAN et al., 2008). The rhyolite of Rupnica and the Mt. Požeška Gora granite share their age with those of *banatites* and therefore could represent the westernmost occurrences of the BMMB, as has been previously suggested by ILINCA et al. (2011). This opens a new link and possible extension of research in the future, because the relationship between the BMMB and the igneous rocks, which penetrated the Sava Zone and Tisia Mega-Unit in the south-western part of the Panonian basin, is currently far from clear.

## 6. CONCLUSION

The chemical compositions of zircon, apatite, and whole-rock, as well as the petrography of the rhyolite of Rupnica indicate that the magma forming this rock originated from partial melting of mid- to lower-continental crust at temperatures > 800 °C. The compressional tectonics of the Adria microplate towards Europe and the closure of the Neotethys Ocean caused the opening of local extensional zones. In such a tectonic environment, the magmas of the rhyolite of Rupnica were generated. These local extensional zones acted as pathways for the rapid ascent of hot, dry, and oxidized acidic magmas to (sub)surface levels in the Late Cretaceous at ca. 81 Ma. The rhyolite of Rupnica and the granite from Mt. Požeška Gora have similar geochemical characteristics; both rocks formed contemporaneously from peraluminous, ferroan, alkali-calcic to alkalic A-type magmas of the same origin. The Cretaceous (ca. 81 Ma) magmas intruded the Sava Zone and the adjacent Tisia Mega-Unit.

## ACKNOWLEDGMENT

The authors are grateful to Jarmila LUPTAKOVA (†) for her help with Raman spectroscopy. The support with logistics provided by the Papuk Nature Park and Goran RADONIĆ is greatly ap-

preciated. Our gratitude goes to Ralf SCHUSTER and Vladica CVETKOVIĆ for their constructive comments and Vesnica GARAŠIĆ for editorial handling. Support by the Croatian Science Foundation (IP 2014-09-9541) is acknowledged.

## REFERENCES

- BALEN, D. & BROSKA, I. (2011): Tourmaline nodules: products of devolatilization within the final evolutionary stage of granitic melt?– *Geol. Soc. London Spec. Publ.*, 350, 53–68. doi: 10.1144/SP350.4
- BALEN, D. & PETRINEC, Z. (2011): Contrasting tourmaline types from peraluminous granites: a case study from Moslavačka Gora (Croatia).– *Mineral. Petrol.*, 102, 117–134. doi: 10.1007/s00710-011-0164-8
- BALEN, D. & PETRINEC, Z. (2014): Development of columnar jointing in albite rhyolite in a rapidly cooling volcanic environment (Rupnica, Papuk Geopark, Croatia).– *Terra Nova*, 26, 102–110. doi: 10.1111/ter.12075
- BALEN, D., SCHUSTER, R., GARAŠIĆ, V. & MAJER, V. (2003): The Kamenjača olivine gabbro from Moslavačka Gora (South Tisia, Croatia).– *Rad Hrvatske Akademije Znanosti i Umjetnosti*, 48, 27, 57–76.
- BALEN, D., HORVATH, P., TOMLJENIČIĆ, B., FINGER, F., HUMER, B., PAMIĆ, J. & ARKAL, P. (2006): A record of pre-Variscan Barrovian regional metamorphism in the eastern part of the Slavonian Mountains (NE Croatia).– *Mineral. Petrol.*, 87/1, 143–162. doi: 10.1007/s00710-006-0120-1
- BALEN, D., HORVÁTH, P., FINGER, F. & STARJAJŠ, B. (2013): Phase equilibrium, geothermobarometric and xenotime age dating constraints on the Alpine metamorphism recorded in chloritoid schists from the southern part of the Tisia Mega-Unit (Slavonian Mts., NE Croatia).– *Int. J. Earth Sci. (Geol. Rundsch.)*, 102, 1091–1109. doi: 10.1007/s00531-012-0850-8
- BALEN, D., MASSONNE, H.-J. & PETRINEC, Z. (2015): Collision-related Early Paleozoic evolution of a crustal fragment from the northern Gondwana margin (Slavonian Mountains, Tisia Mega-Unit, Croatia): Reconstruction of the P–T path, timing and paleotectonic implications.– *Lithos*, 232, 211–228. doi: 10.1016/j.lithos.2015.07.003
- BALEN, D., MASSONNE, H.-J. & LIHTER, I. (2018): Alpine metamorphism of low-grade schists from the Slavonian Mountains (Croatia): new P–T and geochronological constraints.– *Int. Geol. Rev.*, 60/3, 288–304. doi: 10.1080/00206814.2017.1328710
- BALEN, D., SCHNEIDER, P., MASSONNE, H.-J., OPITZ, J., LUPTAKOVA, J., PUTIŠ, M. & PETRINEC, Z. (2020): The Late Cretaceous A-type alkali-feldspar granite from Mt. Požeška Gora (N Croatia): Potential marker of fast magma ascent in the Europe–Adria suture zone.– *Geol. Charpath.*, 71/4, 361–381. doi: 10.31577/Geol-Carp.71.4.5
- BATCHELOR, R. A. & BOWDEN, P. (1985): Petrogenetic interpretation of granitoid rock series using multicationic parameters.– *Chem. Geol.*, 48, 43–55. doi: 10.1016/0009-2541(85)90034-8
- BAU, M. (1996): Controls on the fractionation of isovalent trace elements in magmatic and aqueous systems: evidence from Y/Ho, Zr/Hf, and lanthanide tetrad effect.– *Contrib. Mineral. Petrol.*, 123, 323–333. doi:10.1007/s004100050159
- BELAK, M., MIKNIĆ, M., KRUK, B., KASTMULLER, Ž. & KRUK, L.J. (2000): Bazalt-glinoviti peperiti: litofacijsni i kronostratigrafski prinos poznavanju vulkanita Budima kod Voćina [Basalt-clayey limestone peperites: Lithofacies and chronostratigraphic contribution to the knowledge of the volcanites of the Mt. Budim near Voćin – in Croatian, with an English abstract].– *Zbornik radova, 2. Hrvatski geološki kongres, Institut za geološka istraživanja*, 109–113.
- BELOUSOVA, E.A., WALTERS, S., GRIFFIN, W.L., O'REILLY, S.Y. & FISHER, N.I. (2002a): Igneous zircon: trace element composition as an indicator of source rock type.– *Contrib. Mineral. Petrol.*, 143, 602–622. doi: 10.1007/s00410-002-0364-7
- BELOUSOVA, E.A., GRIFFIN, W.L., O'REILLY, S.Y. & FISHER, N.I. (2002b): Apatite as an indicator mineral for mineral exploration: Trace-element compositions and their relationship to host rock type.– *J. Geochem. Explor.*, 76, 45–69. doi: 10.1016/S0375-6742(02)00204-2
- BERZA, T., CONSTANTINESCU, E. & VLAD, Ș.N. (1998): Upper Cretaceous magmatic series and associated mineralization in the Carpathian–Balkan Orogen.– *Resour. Geol.*, 48, 291–306. doi: 10.2478/s13386-011-0023-8
- BIŠEVAC, V., BALOGH, K., BALEN, D. & TIBLJAŠ, D. (2010): Alpine (Cretaceous) very low- to low-grade metamorphism recorded on the illite-muscovite-rich fraction of metasediments from South Tisia (eastern Mt Papuk, Croatia).– *Geol. Carpath.*, 61, 469–481.
- BOYNTON, W.V. (1984): Geochemistry of the rare earth elements: meteorite studies.– In: HENDERSON, P. (ed.): *Rare earth element geochemistry*. Elsevier, 63–114.
- BREITER, K. & ŠKODA, R. (2017): Zircon and whole-rock Zr/Hf ratios as markers of the evolution of granitic magmas: Examples from the Teplce caldera (Czech Republic/Germany).– *Mineral. Petrol.*, 111, 435–457. doi: 10.1007/s00710-017-0509-z

- BUROV, E., GUILLOU-FROTTIER, L., D'ACREMON, E., LE POURHIET, L. & CLOETINGH, S. (2007): Plume head–lithosphere interactions near intra-continental plate boundaries.– *Tectonophys.*, 434, 15–38. doi:10.1016/j.tecto.2007.01.002
- CROATIAN GEOLOGICAL SURVEY (2009): Geological Map of the Republic of Croatia, 1:300.000 (Geološka karta Republike Hrvatske).– Croatian Geological Survey, Department of Geology, Zagreb (in Croatian).
- CVETKOVIĆ, V., ŠARIĆ, K., GRUBIĆ, A., CVJIJIĆ, R. & MILOŠEVIĆ, A. (2014): The Upper Cretaceous ophiolite of North Kozara – remnants of an anomalous mid-ocean ridge segment of the Neotethys?– *Geol. Carpath.*, 65, 117–130. doi: 10.2478/geoca-2014-0008
- DE LA ROCHE, H., LETERRIER, J., GRANDCLAUDE, P. & MARCHAL, M. (1980): A classification of volcanic and plutonic rocks using R1R2-diagram and major element analyses – its relationships with current nomenclature.– *Chem. Geol.*, 29, 183–210. doi: 10.1016/0009-2541(80)90020-0
- DICKINSON, W. & GEHRELS, G. (2003): U–Pb ages of detrital zircons from Permian and Jurassic eolian sandstones of the Colorado Plateau, USA: paleogeographic implications.– *Sediment. Geol.*, 163, 29–66. doi: 10.1016/S0037-0738(03)00158-1
- EBY, G.N. (1990): The A-type granitoids: a review of their occurrence and chemical characteristics and speculations on their petrogenesis.– *Lithos*, 26, 115–134. doi:10.1016/0024-4937(90)90043-Z
- EBY, G.N. (1992): Chemical subdivision of the A-type granitoids: petrogenetic and tectonic implications.– *Geology*, 20, 641–644.
- ERDMANN, S., WODICKA, N., JACKSON, S.E. & CORRIGAN, D. (2013): Zircon textures and composition refractory recorders of magmatic volatile evolution?– *Contrib. Mineral. Petr.*, 165, 45–71. doi: 10.1007/s00410-012-0791-z
- FREZZOTTI, M.L., TECCE, F. & CASGALI, A. (2012): Raman spectroscopy for fluid inclusions analysis.– *J. Geochem. Explor.*, 112, 1–12. doi: 10.1016/j.gexplo.2011.09.009
- FROST, C.D. & FROST, B.R. (2011): On ferroan (A-type) granitoids: their compositional variability and modes of origin.– *J. Petrol.*, 32, 39–53. doi: org/10.1093/petrology/egq070
- FROST, B.R., BRANES, C.G., COLLINS, W.J., ARCULUS, R.J., ELLIS, D.J. & FROST, C.D. (2001): A geochemical classification for granitic rocks.– *J. Petrol.*, 42, 2033–2048. doi: 10.1093/petrology/42.11.2033
- FU, B., PAGE, F.Z., CAVOSIE, J.C., FOURNELLE, J., KITA, N.T., LACKEY, J.S., WILDE, S.A. & VALLEY, J.W. (2008): Ti-in-zircon thermometry: applications and limitations.– *Contrib. Mineral. Petr.*, 156, 197–215. doi: 10.1007/s00410-008-0281-5
- GERVASONI, F., KLEMME, S., ROCHA-JÚNIOR, E.R.V. & BERNDT, J. (2016): Zircon saturation in silicate melts: a new and improved model for aluminous and alkaline melts.– *Contrib. Mineral. Petr.*, 171, 21. doi: 10.1007/s00410-016-1227-y
- HARRIS, N.B.W., PEARCE, J.A. & TINDLE, A.G. (1986): Geochemical characteristics of collision-zone magmatism.– In: COWARD, M.P. & RIES, A.C. (eds): *Collision Tectonics*.– *Geol. Soc. London Spec. Publ.*, 19, 67–81.
- HARRISON, T.M. & WATSON, E.B. (1984): The behavior of apatite during crustal anatexis: Equilibrium and kinetic considerations.– *Geochim. Cosmochim. Acta*, 48, 1467–1477. doi: 10.1016/0016-7037(84)90403-4
- HOSKIN, P.W.O. & SCHALTEGGER, U. (2003): The composition of zircon and igneous and metamorphic petrogenesis.– *Rev. Mineral. Geochem.*, 53, 27–62. doi: 10.2113/0530027
- HOSKIN, P.W.O., KINNY, P.D., WYBORN, D. & CHAPPELL, B.W. (2000): Identifying Accessory Mineral Saturation during Differentiation in Granitoid Magmas: an Integrated Approach.– *J. Petrol.*, 41/9, 1365–1396. doi: 10.1093/petrology/41.9.1365
- HORVÁTH, P., BALEN, B., FINGER, F., TOMLJENIĆ, B. & KRENN, E. (2010): Contrasting P–T–t paths from the basement of the Tisia Unit (Slavonian Mts., NE Croatia): application of quantitative phase diagrams and monazite age dating.– *Lithos*, 117, 269–282. doi: 10.1016/j.lithos.2010.03.004
- HORVAT, M., KLÖTZLI, U., JAMIČIĆ, D., BUDA, G., KLÖTZLI, E. & HAUZENBERGER, CH. (2018): Geochronology of granitoids from Pšunj and Papuk Mts., Croatia.– *Geochronometria*, 45/1, 198–210. doi: 10.1515/geochr-2015-0099
- HURAI V., HURAIIOVÁ, M., SLOBODNÍK, M. & THOMAS R. (2015): Geofluids – Developments in Microthermometry, Spectroscopy, Thermodynamics, and Stable Isotopes.– Elsevier, Amsterdam, 489 p.
- ILINCA, G., BERZA, T., IANCU, V. & SEGHEDI, A. (2011): Field Trip Guidebook, The Late Cretaceous Magmatic and Metallogenetic Belt and the Alpine structures of the western South Carpathians. 3<sup>rd</sup> International Symposium on the Geology of the Black Sea Region, Bucharest, 1–10 October 2011, 117 p.
- JAMIČIĆ, D. (1983): Strukturni sklop metamorfnih stijena Krndije i južnih padina Papuka [*Structural fabric of the metamorphosed rocks of Mt. Krndija and the eastern part of Mt. Papuk* – in Croatian, with an English summary].– *Geol. vjesnik*, 36, 51–72.
- JAMIČIĆ, D. (1988): Strukturni sklop slavonskih planina [*Structural fabric of the Slavonian Mts. (northern Papuk, Pšunj, Krndija)* – in Croatian, with an English summary].– PhD Thesis, Faculty of Science, University of Zagreb, 152 p.
- JAMIČIĆ, D. (1989): Osnovna geološka karta SFRJ 1:100000, list Daruvar L 33-95 [*Basic Geological Map of SFRJ 1:100000, Daruvar sheet* – in Croatian].– Geološki zavod, Zagreb, Savezni geološki zavod, Beograd.
- JAMIČIĆ, D. & BRKIĆ, M. (1986): Osnovna geološka karta SFRJ 1:100000, list Orahovica L 33-96 [*Basic Geological Map of SFRJ 1:100000, Orahovica sheet* – in Croatian].– Geološki zavod, Zagreb, Savezni geološki zavod, Beograd.
- JAMIČIĆ, D., BRKIĆ, M., CRNKO, J. & VRAGOVIĆ, M. (1987): Osnovna geološka karta SFRJ 1:100000. Tumač za list Orahovica L 33-96 [*Basic Geological Map of SFRJ 1:100000, Geology of the Orahovica sheet* – in Croatian].– Geološki zavod, Zagreb, Savezni geološki zavod, Beograd, 72 p.
- JAMIČIĆ, D., VRAGOVIĆ, M. & MATIČEĆ, D. (1989): Osnovna geološka karta SFRJ 1:100000. Tumač za list Daruvar L 33-95 [*Basic Geological Map of SFRJ 1:100000, Geology of the Daruvar sheet* – in Croatian].– Geološki zavod, Zagreb, Savezni geološki zavod, Beograd, 55 p.
- JANOŠEK, V., FARROW, C.M. & ERBAN, V. (2006): Interpretation of whole-rock geochemical data in igneous geochemistry: introducing Geochemical Data Toolkit (GCDkit).– *J. Petrol.*, 47, 1255–1259. doi: 10.1093/petrology/egl013
- KEMPTON, P.D., HARMON, R.S., HAWKESWORTH, C.J. & MOORBATH, S. (1990): Petrology and geochemistry of lower crustal granulites from the Geronimo Volcanic Field, southeastern Arizona.– *Geochim. Cosmochim. Acta*, 54, 3401–3426. doi:10.1016/0016-7037(90)90294-U
- KING, P.L., WHITE, A.J.R., CHAPPELL, B.W. & ALLEN, C.M. (1997): Characterization and origin of aluminous a-type granites from the Lachlan Fold Belt, Southeastern Australia.– *J. Petrol.*, 38, 371–391. doi: 10.1093/petroj/38.3.371
- KIRKLAND, C.L., SMITHIES, R.H., TAYLOR, R.J.M., EVANS, N. & MCDONALD, B. (2015): Zircon Th/U ratios in magmatic enviroins.– *Lithos*, 212–215, 397–414. doi: 10.1016/j.lithos.2014.11.021
- KOCH, F. (1919): Grundlinien der Geologie von West-Slavonien.– *Glasnik hrv. prir. dr.*, 31/2, 217–236.
- LUGOVIĆ, B. (1983): Efuzivne stijene sjeverozapadnog dijela Papuka. [*Extrusive rocks from the NW part of Mt. Papuk (Croatia, Yugoslavia)* – in Croatian, with an English summary].– *Geol. vjesnik*, 36, 131–156.
- LUŽAR-ÖBERITER, B., MIKES, T., DUNKL, I., BABIĆ, L.J. & VON EYNATTEN, H. (2012): Provenance of Cretaceous synorogenic sediments from the NW Dinarides (Croatia).– *Swiss J. Geosci.*, 105, 377–399. doi: 10.1007/s00015-012-0107-3
- MCLENNAN, S.M. (1994): Rare earth element geochemistry and the “tetrad” effect.– *Geochim. Cosmochim. Acta*, 58, 2025–2033. doi:10.1016/0016-7037(94)90282-8
- PACES, J.B. & MILLER, J.D. (1993): Precise U–Pb ages of Duluth Complex and related mafic intrusions, northeastern Minnesota: geochemical insights into physical, petrogenetic, paleomagnetic and tectonomagmatic processes associated with the 1.1 Ga midcontinent rift system.– *J. Geophys. Res.*, 98, 13997–14013. doi: 10.1029/93JB01159
- PAMIĆ, J. (1987): Mladoalpinski alkalijsko-feldspatski graniti (aljskiti) Požeške gore u Slavoniji [*Young-Alpine alkali feldspar granites (alaskites) from Mt. Požeška Gora in Slavonia, northern Yugoslavia* – in Croatian, with English summary].– *Geologija*, 30, 183–205.
- PAMIĆ, J. (1991): Gornjokredne bazaltoidne i piroklastične stijene iz voćinske vulkanske mase na Papuku (Slavonija, sj. Hrvatska) [*Upper Cretaceous basaltoid and pyroclastic rocks from the Voćin volcanic mass on the Papuk Mt. (Slavonija, Northern Croatia)* – in Croatian, with an English summary].– *Geol. vjesnik*, 44, 161–172.
- PAMIĆ, J. (1993): Eoalpine to Neoalpine magmatic and metamorphic processes in the northwestern Vardar Zone, the easternmost Periadriatic Zone and the southwestern Pannonian Basin.– *Tectonophysics*, 109, 273–307. doi: 10.1016/0040-1951(93)90135-7
- PAMIĆ, J. (1997): Vulkanske stijene Savsko-dravskog međuriječja i Baranje (Hrvatska) [*Volcanic rocks of the Sava-Drava interfluvium and Baranja (Croatia)* – in Croatian, with English summary].– *Nafta*, Zagreb, 192 p.
- PAMIĆ, J. (2002): The Sava-Vardar Zone of the Dinarides and Hellenides versus the Vardar Ocean.– *Eclogae Geol. Helv.*, 95, 99–113. doi: 10.5169/seals-168948
- PAMIĆ, J. & INJUK, J. (1988): Alpske granitoidne stijene Prosare u sjevernoj Bosni.– *Zbor. ref. nauč. skupa “Minerali, stijene, izumrl i živi svijet BiH”*, 93–103, Sarajevo.
- PAMIĆ, J. & LANPHERE, M. (1991a): Hercynian granites and metamorphic rocks from the Papuk, Pšunj, Krndija and the surrounding basement of the Pannonian Basin (Northern Croatia, Yugoslavia).– *Geologija*, 34, 81–253.
- PAMIĆ, J. & LANPHERE, M. (1991b): A-type granites from the collisional area of the northernmost Dinarides and Pannonian Basin. *Neues Jahrb. Mineral. Abh.*, 161, 215–236.
- PAMIĆ, J., LANPHERE, M. & MCKEE, E. (1988): Radiometric ages of metamorphic and associated igneous rocks of the Slavonian Mountains in the southern part of the Pannonian basin.– *Acta Geol.*, 18, 13–39.
- PAMIĆ, J., INJUK, J. & JAKŠIĆ, M. (1988/1989): Prilog geokemijskom poznavanju gornjokredne bimodalne vulkanske asocijacije Požeške gore u Slavoniji (Sjeverna Hrvatska, Jugoslavija) [*Some geochemical features of the Upper Cretaceous bimodal volcanic association from the Požeška Gore Mt. in Slavonija (northern Croatia, Yugoslavia)* – in Croatian, with an English summary].– *Geologija*, 31–32, 415–435.

- PATIÑO DOUCE, A.E. (1997): Generation of metaluminous A-type granites by low-pressure melting of calc-alkaline granitoids.– *Geology*, 25, 743–746. doi:10.1130/0091-7613
- PICCOLI, P.M. & CANDELA, P.A. (1994): Apatite in felsic rocks: a model for the estimation of initial halogen concentrations in the Bishop Tuff (Long Valley) and Tolumne Intrusive Suite (Sierra Nevada Batholith) magmas.– *Am. J. Sci.*, 294, 92–135. doi: 10.2475/ajs.294.1.92
- PICCOLI, P.M. & CANDELA, P.A. (2002): Apatite in Igneous Systems.– *Rev. Mineral. Geochem.*, 48, 255–292. doi: 10.2138/rmg.2002.48.6
- PEARCE, J.A. (1996): Sources and settings of granitic rocks.– *Episodes*, 19, 120–125. doi: 10.18814/epiugs/1996/v19i4/005
- PEARCE, J.A., HARRIS, N.B.W. & TINDLE, A.G. (1984): Trace element discrimination diagrams for the tectonic interpretation of rhyolitic rocks.– *J. Petrol.*, 25, 956–981.
- POLJAK, J. (1939): Izvještaj o geološkom snimanju lista Slatina-Voćin (1:25.000).– *Godišnjak Geol. inst. Kr. Jug.* 1938, 1, 89–92, Beograd (in Croatian).
- PUPIN, J.P. (1980): Zircon and granite petrology.– *Contrib. Mineral. Petr.*, 73, 207–220. doi: 10.1007/BF00381441
- PUPIN, J.P. (2000): Granite genesis related to geodynamics from Hf-Y in zircon.– *Trans. R. Soc. Edinburgh: Earth Sci.*, 91, 245–256. doi: 10.1017/S0263593300007410
- PUPIN, J.P. & TURCO, G. (1972): Une typologie originale du zircon accessoire.– *Bull. Soc. Fr. Minéral. Cristallogr.*, 95, 348–359.
- SCHILLER, D. & FINGER, F. (2019): Application of Ti-in-zircon thermometry to granite studies: problems and possible solutions.– *Contrib. Mineral. Petr.*, 174, 51. doi: 10.1007/s00410-019-1585-3
- SCHMID, S.M., BERNOULLI, D., FÜGENSCHUH, B., MATENCO, L., SCHEFER, S., SCHUSTER, R., TISCHLER, M. & USTASZEWSKI, K. (2008): The Alps–Carpathians–Dinarides connection: a compilation of tectonic units.– *Swiss J. Geosci.*, 101, 139–183. doi: 10.1007/s00015-008-1247-3
- SCHMID, S.M., FÜGENSCHUH, B., KOUNOV, A., MAŢENCO, L., NIEVERGELT, P., OBERHÄNSLI, R., PLEUGER, J., SCHEFER, S., SCHUSTER, R., TOMLJENOVIC, B., USTASZEWSKI, K. & VAN HINSBERGEN, D.J.J. (2020): Tectonic units of the Alpine collision zone between Eastern Alps and western Turkey.– *Gondwana Res.*, 78, 308–374. doi: 10.1016/j.gr.2019.07.005
- SHAULIS, B., LAPEN, T.J. & TOMS, A. (2010): Signal linearity of an extended range pulse counting detector: Applications to accurate and precise U-Pb dating of zircon by laser ablation quadrupole ICPMS.– *Geochem. Geophys. Geosyst.*, 11, Q0AA11. doi: 10.1029/2010GC003198
- SKJERLIE, K.P. & JOHANSON, A.D. (1993): Fluid-absent melting behavior of an F-rich tonalitic gneiss at mid-crustal pressures: implications for the generation of anorogenic granites.– *J. Petrol.*, 34, 785–815. doi:10.1093/petrology/34.4.785
- SLÁMA, J., KOSLER, J., CONDON, D.J., CROWLEY, J.L., GERDES, A., HANCHAR, J.M., HORSTWOOD, M.S.A., MORRIS, G.A., NASDALA, L., NORBERG, N., SCHALTEGGER, U., SCHOENE, N., TUBRETT, M.N. & WHITEHOUSE, M.J. (2008): Plesovice zircon – a new natural reference material for U–Pb and Hf isotopic microanalysis.– *Chem. Geol.*, 249, 1–35. doi: 10.1016/j.chemgeo.2007.11.005
- SŁODCZYK, E., PIETRANIK, A., BREITKREUZ, C., FANNING, C., ANCKIEWICZ, R., EHLING, B.-C. (2016): Rhyolite magma evolution recorded in isotope and trace element composition of zircon from Halle Volcanic Complex.– *Lithos*, 248–251, 402–417. doi: 10.1016/j.lithos.2016.01.029
- SLOVENEČ, D., BELAK, M., MIŠUR, I., ŠEGVIĆ, B. & SCHUSTER, R. (2020): The early Paleozoic cumulate gabbroic rocks from the southwest part of the Tisza Mega-Unit (Mt. Papuk, NE Croatia): evidence of a Gondwana suture zone.– *Int. J. Earth. Sci. (Geol. Rundsch.)*, 109, 2209–2233. doi: 10.1007/s00531-020-01896-8
- STARIJAŠ, B., GERDES, A., BALEN, D., TIBLJAŠ, D. & FINGER, F. (2010): The Moslavačka Gora crystalline massif in Croatia: a Cretaceous heat dome within remnant Ordovician granitoid crust.– *Swiss. J. Geosci.*, 103, 61–82. doi: 10.1007/s00015-010-0007-3
- STRECKEISEN, A. (1974): Classification and nomenclature of plutonic rocks.– *Geol. Rundsch.*, 63, 773–786.
- STRECKEISEN, A. (1978): IUGS Subcommittee on the Systematics of Igneous Rocks: Classification and nomenclature of volcanic rocks, lamprophyres, carbonatites and melilitic rocks; recommendation and suggestions.– *Neues Jb. Mineral Abh.*, 134, 1–14.
- STUR, D. (1861/62): Die neogen tertiären Ablagerungen von West Slavonien.– *Jahrb. Reichanst.*, 12, 285–299.
- SUN, S.S. & MCDONOUGH, W.F. (1989): Chemical and isotopic systematics of oceanic basalts: implications for mantle composition and processes.– In: SAUNDERS, A.D. & NORRY, M.J. (eds.): *Magmatism in ocean basins.*– *Geol. Soc. Spec. Publ.*, 42, 313–345. doi: 10.1144/GSL.SP.1989.042.01.19
- TAJDER, M. (1956): Albitski efuzivi okolice Voćina i njihova geneza [*The albite volcanic rocks of the Voćin area and their origin*] – in Croatian, with an English summary].– *Acta geol.* 1 (Prir. istraž. JAZU), 27, 35–48.
- TAJDER, M. (1960): Anortoklasni egirinski riolit iz potoka Rupnice kod Voćina [*Anorthoclase-aegirine-rhyolite from Rupnica brook near Voćin*] – in Croatian, with an English summary].– *Acta geol.* 2 (Prir. istraž. JAZU), 29, 95–101.
- USTASZEWSKI, K., SCHMID, S.M., LUGOVIĆ, B., SCHUSTER, R., SCHALTEGGER, U., BERNOULLI, D., HOTTINGER, L., KOUNOV, A., FÜGENSCHUH, B. & SCHEFER, S. (2009): Late Cretaceous intra-oceanic magmatism in the internal Dinarides (northern Bosnia and Herzegovina): implications for the collision of the Adriatic and European plates.– *Lithos*, 108, 106–125. doi: 10.1016/j.lithos.2008.09.010
- USTASZEWSKI, K., KOUNOV, A., SCHMID, S.M., SCHALTEGGER, U., KRENN, E., FRANK, W. & FÜGENSCHUH, B. (2010): Evolution of the Adria–Europe plate boundary in the northern Dinarides: from continent–continent collision to back-arc extension.– *Tectonics*, 29, TC6017. doi: 10.1029/2010TC002668
- WANG, X., GRIFFIN, W.L. & CHEN, J. (2010): Hf contents and Zr/Hf ratios in granitic zircons.– *Geochem. J.*, 44, 65–72. doi: 10.2343/geochemj.1.0043
- WATSON, E.B. & HARISSON, T.M. (1983): Zircon saturation revisited: temperature and composition effects in a variety of crustal magma types.– *Earth Planet. Sci. Lett.*, 64, 295–304. doi: 10.1016/0012-821X(83)90211-X
- WATSON, E.B., WARK, D.A. & THOMAS, J.B. (2006): Crystallization thermometers for zircon and rutile.– *Contrib. Mineral. Petr.*, 151, 413–433. doi: 10.1007/s00410-006-0068-5
- WHALEN, J.B., CURRIE, K.L. & CHAPPELL, B.W. (1987): A-type granites: geochemical characteristics, discrimination and petrogenesis.– *Contrib. Mineral. Petr.*, 95, 407–419. doi: 10.1007/BF00402202
- ZIMMERMAN, A., STEIN, H.J., HANNAH, J.L., KOŽELJ, D., BOGDANOV, K. & BERZA, T. (2008): Tectonic configuration of the Apuseni–Banat–Timok–Srednogorie belt, Balkans–South Carpathians, constrained by high precision RE–OS molybdenite ages.– *Miner. Deposita*, 43/1, 1–21. doi: 10.1007/s00126-007-0149-z